
PROJECT SUMMARY: Collaborative Research:
The kinematics, microphysics and dynamics of long-fetch lake-effect systems in OWLeS

This collaborative proposal is one of three centered on the Ontario Winter (OW) Lake-effect Systems (LeS) field campaign, scheduled for Dec. 2013 – Jan. 2014. The OWLeS campaign aims to document dynamical and cloud microphysical processes of planetary boundary-layer (PBL) convection over and downstream of relatively warm, mesoscale open-water surfaces at unprecedented detail, using X-band and S-band dual-polarization (dual-pol) radars, an aircraft instrumented with particle probes and profiling cloud radar and lidar, a mobile integrated sounding system, a network of radiosondes, and a surface network of snow characterization instruments. The OWLeS project focuses on Lake Ontario because of its size and orientation, the frequency of LeS events (especially intense single bands), its nearby moderate orography, the impact of Lake Ontario LeS hazards in particular on public safety and commerce, and the proximity of several universities with large atmospheric science programs. The OWLeS project distinguishes between two primary modes, depending on prevailing wind direction: 1) short-fetch LeS (those oriented at large angles to the long axis of the lake), that are addressed by a companion proposal; and, 2) long-fetch LeS (those more aligned with the lake's long axis), that are the main topic of this proposal. The 3rd proposal focuses on downstream coastal and orographic effects. The PIs of the three proposals are committed to coordinated field operations, the sharing of all OWLeS data and analysis products, and collaborative research.

This proposal and the OWLeS project stand out mainly for two reasons: 1) the focus on physical processes in the context of a prime example of interactions between the PBL, the surface, and cloud & precipitation, interactions that current operational numerical weather prediction (NWP) and climate models cannot resolve because the processes are separately parameterized; and 2) the unique collaboration with undergraduate programs at several universities and the extensive opportunities for undergraduate students to participate in cutting-edge research all the way from data collection in the field to peer-reviewed publications.

The key scientific objectives of this proposal are to describe and understand: 1) how long-fetch LeS intensify and evolve downwind of the lake; 2) fine-scale cloud and dynamical processes in long-fetch LeS, including the observed occasional lightning; 3) how radar dual-pol variables at X- and S-band reveal precipitation processes in LeS, and how well dual-pol particle identification and QPE (quantitative precipitation estimation) algorithms perform in LeS.

Intellectual merit. While current operational NWP models reasonably capture LeS timing, predictions of the amounts and inland extent of LeS snowfall remain poor. Likely causes of poor QPF (quantitative precipitation forecasting) of LeS include not merely model resolution, but also fine-scale variations in upwind PBL structure and poor representation of cloud microphysical, dynamical, and surface processes. Building on previous LeS field campaigns, the OWLeS project will not only document the thermodynamic, kinematic, and cloud microphysical structure of LeS at unprecedented resolution, but will also further our understanding of key processes in LeS by deploying a mesoscale network of new, high-resolution *in situ* and remote sensors. This network is well suited not only to capture the structure, evolution, and spatio-temporal variability of LeS, but also to evaluate and assess the hydrometeor classification and QPE algorithms for the recently dual-pol upgraded WSR-88D radars, which has not been done for lake-effect snowfall, and for cold-season systems in general.

Broader Impacts. Lake-effect snow events create major weather hazards downwind of the Great Lakes. The critical parameters are fine-scale, real-time QPE and QPF. The OWLeS research aims to accomplish improved QPE and QPF, the latter by means of a better understanding of relevant physical processes. This research becomes more urgent in a warming global climate, as boreal lakes and the Arctic coastal waters are expected to remain ice-free for longer periods. This may lead to substantial increases in boundary-layer heat, moisture and snow growth, especially early in the cold season, and, as a result, an increase in coastal erosion, precipitation, and ecosystem impacts. Finally, the OWLeS campaign will offer many students, mostly undergraduates, training opportunities in hands-on instrument-based end-to-end (data to papers) research in atmospheric science, and will reach out to numerous K-12 students.

The kinematics, microphysics and dynamics of long-fetch lake-effect systems in OWLeS

1. Background

1.1 The OWLeS project

The Ontario Winter Lake-effect Systems (OWLeS) project is centered on a collaborative field campaign, to be conducted in the winter of 2013-14 in the vicinity of Lake Ontario. The campaign will host a number of NSF-supported as well as participant-supplied facilities, in particular the University of Wyoming King Air (UWKA), two dual-pol (short for dual-polarization) and a rapid-scan Doppler-on-Wheels (DOW) X-band mobile radars, 5 mobile rawinsonde systems, the Millersville University Profiling System (MUPS) and the University of Alabama Huntsville (UAH) Mobile Integrated Profiling System (MIPS).

The OWLeS team includes the PIs on this proposal [*Bart Geerts* – UW; *Kevin Knupp* – UAH; *Karen Kosiba* & *Joshua Wurman* – Center for Severe Weather Research (CSWR); *Scott Steiger* – State University of New York Oswego (SUNY-Oswego); and *Jeff Frame* - Univ. of Illinois (UIUC)], plus the PIs on a companion proposal, referred to as OWLeS-SAIL (Surface and Atmospheric Influences on Lake-effect convection). A 3rd independent proposal, referred to as OWLeS-orography, is being submitted by *James Steenburgh* (University of Utah, UU). (This proposal also targets the Great Salt Lake.) The OWLeS-SAIL PIs are *Richard Clark* & *Todd Sikora* - MU, *David Kristovich* - UIUC, *George Young* - Pennsylvania State University; and *Neil Laird* & *Nicholas Metz* - Hobart and William Smith (HWS) Colleges.

The OWLeS project is a comprehensive study of the cloud microphysics and dynamics of lake-effect systems (LeS), with the ultimate objective of improving QPE and QPF of LeS snowfall. The term LeS is used rather than the more common expression "lake-effect snow bands", to be more encompassing. LeS may include cells, singular bands and mesoscale vortices. Their impacts can be felt well inland.

The overall OWLeS project has 7 specific objectives. They are:

1. to understand the development of and interactions between internal layers within the boundary layer (BL) as LeS move over one or more relatively warm bodies of water and intervening land surfaces;
2. to examine how LeS circulations and snowfall are altered by relatively small bodies of open water such as the New York Finger Lakes;
3. to examine how surface fluxes, lake-scale circulations, cloud microphysics and radiative processes affect the formation, structure, and downstream evolution of LeS;
4. to understand how long-fetch LeS (i.e. those aligned with Lake Ontario) intensify and evolve downwind of the lake;
5. to understand cloud and dynamical processes contributing to the occasional lightning observed in long-fetch LeS cells, which may be only a quarter the depth of typical thunderstorms;
6. to examine how radar dual-pol variables at X- and S-band reveal precipitation processes in LeS, and how well dual-pol particle identification and QPE algorithms perform in LeS;
7. to examine the evolution of LeS over elevated terrain downwind of the source lake.

This proposal focuses on objectives 4-6 (highlighted in blue). Several PIs in this proposal will be collaborating on the remaining objectives (see Section 4). OWLeS-SAIL will focus on the first three objectives, and the last objective is the main topic of OWLeS-orography.

1.2 Lake-effect systems

Cells of shallow moist convection commonly are present in the convective BL (CBL). They may form, for instance, when cold air advects over a sufficient fetch of relatively warm water, leading to LeS. Satellite and radar imagery shows that under sufficient wind such cells tend to be linearly organized (e.g., Kelly 1984; Kristovich 1993; Kristovich and Braham 1998; Kristovich et al. 1999; Cooper et al. 2000; Kristovich et al. 2003). Many studies have examined the mechanisms of linear organization [see Etling and Brown (1993) for a review] and have tried to experimentally validate the theoretical aspect ratio (spacing:depth) of cloud streets or snow bands (e.g., Mourad and Brown 1990). The primary linear organization is the result of secondary wind-aligned horizontal vorticity in a sheared CBL; the associated horizontal convective roll (HCR) circulation is sufficient to assemble convective eddies into regularly spaced bands (Young et al. 2002).

Two large field campaigns have focused on LeS over the Great Lakes, using mostly aircraft and radar data (e.g., Braham 1990; Chang and Braham 1991; Kristovich 1993; Braham and Dungey 1995; Kristovich

and Braham 1998; Kristovich et al. 2003): the Lake Ontario Winter Storms (LOWS) project occurred in early 1990 (Reinking et al. 1993), and the Lake-Induced Convection Experiment (Lake-ICE) took place over Lake Michigan in the winter of 1997/98 (Kristovich et al. 2000).

Neither field campaign addressed what we call “**long lake-axis-parallel**” (**LLAP**) snow bands [referred to as Type I by Niziol et al. (1995)], which may form when the prevailing wind blows along the major axis of an elongated lake such as Lake Ontario. In the case of mesoscale lakes such as Lake Ontario, internal dynamics that organize snow bands are compounded by lake-scale circulations: a lake-scale convergent circulation may produce a relatively deep singular snow band leading to persistent heavy snowfall downwind of the lake (e.g., Kristovich and Steve 1995; Niziol et al. 1995). Sometimes such LLAP snow bands become deep enough (tops 3–4 km) to produce lightning (Moore and Orville 1990; Steiger et al. 2009). Even though such bands of heavy snowfall are rather narrow (typically <20 km), under persistent flow they can result in extreme snow accumulations (>1 m depth), resulting in transportation paralysis ((Peace and Sykes 1966; NWS Buffalo 2009a). A recent field study of the fine-scale structure of the LLAP bands (Section 1.3.1) revealed intense cells with features similar to deep convection such as mesovortices, misovortices along shear lines, and bounded weak echo regions (Cermak et al. 2012a; Steiger et al. 2012), which may impact local snowfall amounts. Accurate prediction of the initiation, demise, movement, and intensity of these narrow storms remains elusive (Ballentine and Zaff 2007).

Improved predictability of LeS, including LLAP bands, will not simply result from increased model resolution, but also requires a better understanding of the underlying physical processes. LeS snowfall serves as a fine example of interactions between turbulent flow in the CBL and cloud microphysical processes as well as surface fluxes. These interactions are not represented in operational NWP models. For instance, within the model world, turbulent vertical motions do not affect cloud processes in LeS. This raises the question whether models are right for the wrong reasons.

Several physical processes affecting LeS remain poorly documented or understood. These include lake-to-lake interactions, lake-scale circulations, the fine-scale structure and organization of shallow yet intense LeS convection, and cloud microphysical processes in relatively shallow convection. In addition, little is known about the evolution of LeS across the coast and over downstream terrain. OWLeS will provide a unique opportunity to broaden the understanding of LeS, mainly by deploying and evaluating new high-resolution remote sensing instruments.

Does lake-effect snowfall become less significant in a warming global climate? Its trend actually has been positive around most of the Laurentian Great Lakes in the past century (Burnett et al. 2003; Kunkel et al. 2009). Recently the trend may have reversed (Bard and Kristovich 2012), and it may become more negative later this century, mainly because of weaker cold-air outbreaks (Kunkel et al. 2002). Yet the proposed research becomes more urgent as boreal lakes and the Arctic coastal waters are remaining ice-free for longer periods (e.g., Perovich et al. 2012). This trend is likely to continue into the next few decades (Stroeve et al. 2012), which may lead to substantial increases in boundary-layer heat and moisture fluxes and resultant snow growth, especially early in the cold season, and, as a result, an increase in precipitation, coastal erosion, and ecosystem impacts (Brown and Duguay 2010).

1.3 Intensification and electrification of long-fetch lake-aligned snow bands

1.3.1 *Previous work*

Relatively little is known about the kinematics, dynamics and microphysics of LLAP snow bands such as the one shown in **Fig. 3**. LLAP snow bands are convective and occasionally produce lightning, even though with a cloud top height of 2–4 km, they are far shallower than a typical thunderstorm (Moore and Orville 1990; Steiger et al. 2009). The LOWS Project (Reinking et al. 1993) used a dual-pol X-band radar to investigate lake-effect storms, but analysis was limited to one 4-km deep LLAP-type event, without exploration of the storm’s dual-pol characteristics. The OWLeS capabilities will significantly exceed those in LOWS in terms of the diversity, density and mobility of the proposed instrumentation. The Lake-ICE project (Kristovich et al. 2000) observed one weak lake-effect LLAP event over Lake Michigan (unpublished).

The fine-scale kinematic and microphysical structure of several LLAP bands was examined in a small but successful field campaign called LLAP (winter 2010–11), in which a dual-pol DOW was deployed near the eastern shore of Lake Ontario (PIs Steiger and Frame). Steiger et al. (2012) document well-defined shear boundaries with misovortices in several LLAP band events (**Fig. 1a**). These vortices typically had length

scales of less than 2 km and had radial velocity differences between the couplets of $O(10) \text{ m s}^{-1}$. Other fine-scale BL features were observed such as shallow wind-aligned streaks (Fig. 1b) and mesovortices (Fig. 1c). The strong vertical velocities associated with some features may contribute to the intensification and electrification of LLAP bands. For one LLAP case, on 3 Jan 2011, dual-Doppler synthesis using the DOW and the KTYX Weather Surveillance Radar-88 Doppler (WSR-88D) radars was attempted (Fig. 2a). Due to the coarse spatial and temporal sampling of KTYX and the long baseline (39.4 km), the scales evident in Fig. 1 are not resolved (Fig. 2b), but this analysis provides the foundation for the proposed fine-scale dual- and multi-Doppler analysis.

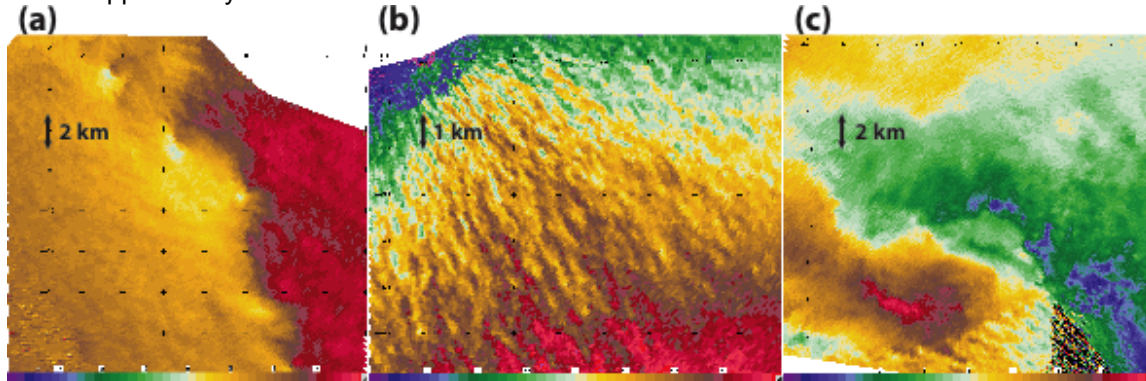


Fig. 1: Examples of different boundary layer features as observed by DOW7 during the LLAP project. Shown is the Doppler velocity for (a) misovortices, (b) boundary layer streaks, and (c) a mesovortex.

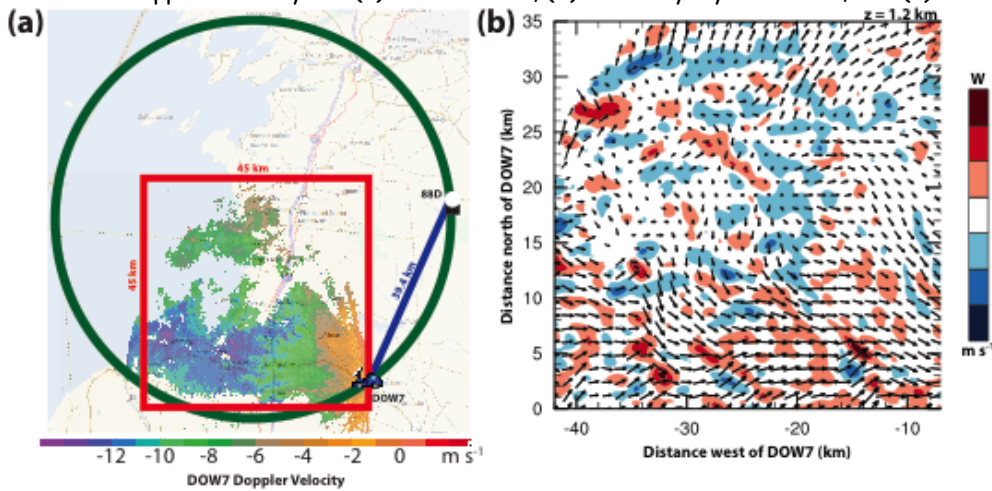


Fig. 2: (a) Dual-Doppler geometry between DOW7 and the KTYX WSR-88D. The green circle indicates the 30° crossing angle and the red box is the dual-Doppler analysis domain. The DOW7 0.5° radial velocity is shown. (b) DOW7-88D dual-Doppler analysis at 1.2 km. Colored contours indicate vertical velocities and vectors display winds. A 3D grid spacing of 400m was used.

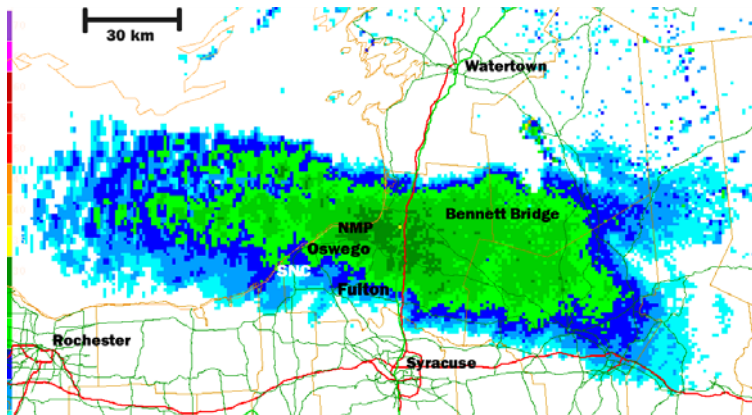


Fig. 3: Base reflectivity (first green contour = 20 dBz, every 5 dBz) from KTYX at 0757 UTC 05 February 2007 for storm 'Locust' (see National Weather Service, Buffalo 2009b).

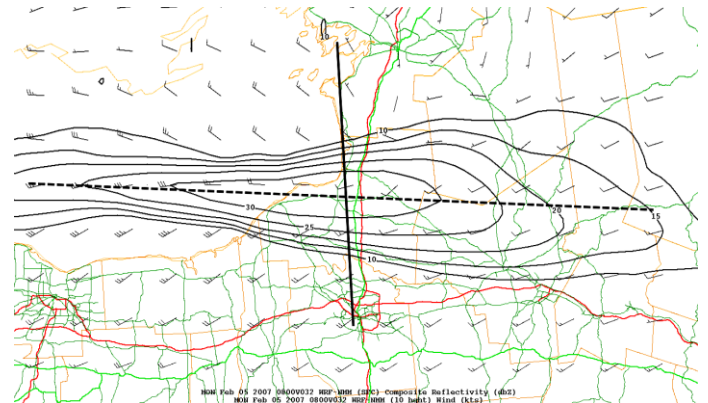


Fig. 4: WRF-simulated composite reflectivity (dBz) and 10-meter wind (kt) at 0800 UTC 05 February 2007 (about the same time as the radar image in Fig. 3). Solid line denotes cross-section shown in Fig. 5.

Cermak et al. (2012a) describe hydrometeor and precipitation growth processes in LLAP bands using the DOW dual-pol data collected during the LLAP campaign (see Section 7.1). This campaign serves as a pilot study for OWLeS, but the outcome is limited because of lack of flight-level measurements, WSR-88D dual-pol data, fine-scale dual-Doppler data, sounding data, and surface snow characterization. Few LLAP band modelling studies have been published (Hjelmfelt 1990; Ballentine et al. 1998). The latter study reveals a distinct transverse mesoscale circulation along LLAP bands, i.e. a solenoidal dipole with convergent flow from opposite shores, rising motion near the center and weaker descent along the edges of the bands. An unpublished simulation of a 2007 LLAP event reveals the same structure (Fig. 4, Fig. 5).

1.3.2 Intensification mechanisms

Surface heat fluxes and lake-scale solenoidal circulation. Sensible and latent heat fluxes from open water increase with at least the square of wind speed (e.g., Drennan et al. 2007). This primary LeS intensification mechanism may be enhanced in the case of LLAP events through stronger surface wind speeds than background flow due to vertical momentum transfer, lake-scale circulations, and small-scale vortical circulations (e.g., Winstead et al. 2001). A rawinsonde pair, one penetrating a LLAP-type band and another outside the band revealed a virtual temperature surplus of 2.5 K inside the snow band (Byrd et al. 1991). Much less buoyancy ($T_v < 0.1$ K) was found in cells of weaker HCR snow bands (Yang and Geerts 2006). Byrd et al. (1991) attribute most of this surplus to enhanced surface sensible heating of the local boundary layer air by the LLAP convergent flow, rather than to latent heat release in cloud (i.e., a parcel temperature excess in the presence of CAPE). The February 2007 WRF simulation also shows a 2-3 K temperature excess inside the simulated snow band (Fig. 5). This solenoidal forcing is the primary driver of the lake-scale secondary circulation. The circulation may be enhanced by shallower land breezes possibly supported by drainage flow from surrounding higher terrain.

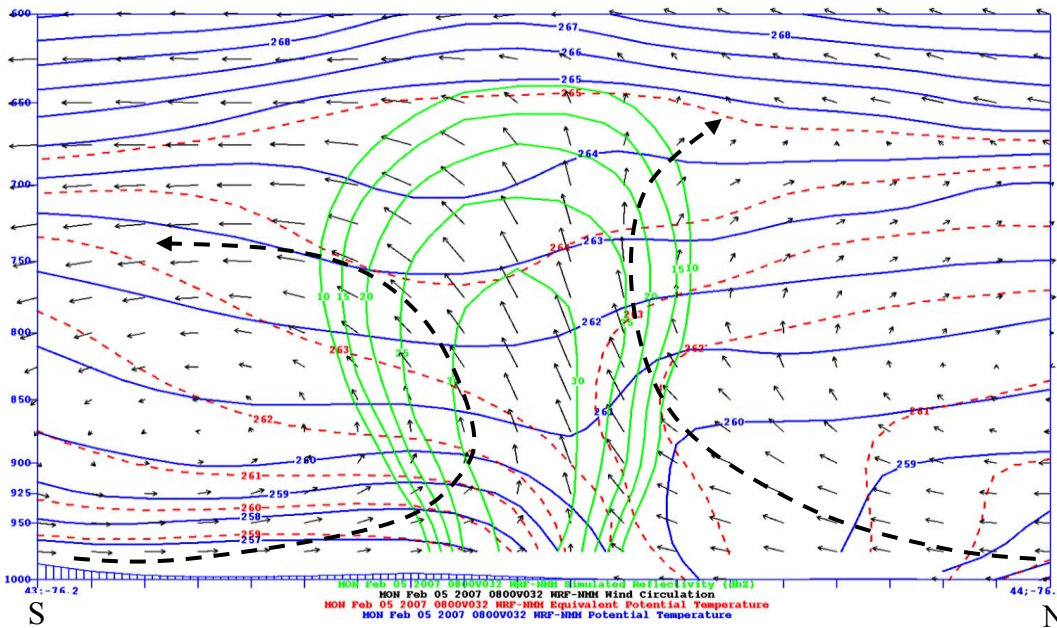


Fig. 5: S-N vertical transect (111 km long) from a WRF simulation of the Locust storm at the same time as in Fig. 4. Shown are potential temperature (K, solid blue), equivalent potential temperature θ_e (K, dashed red), simulated reflectivity (dBz, solid green), and wind on this transect (vectors, with vertical velocity exaggeration matching the plot's $\delta x:\delta z$ ratio).

The dimensions of the lake may impact the intensity of the secondary circulation (Laird et al. 2003). Under lake-parallel flow, the rather small minor axis (50-75 km) of Lake Ontario may allow land breeze currents from opposite shores to coalesce, resulting in a single updraft region. This process is less likely to occur over the western Great Lakes as they are too wide. The lake's length also matters: over a longer lake this solenoidal forcing will have more time to organize the secondary circulation under lake-parallel flow, resulting in more intense LeS snowfall. Mesoscale solenoidal forcing can lead to the development of fine-scale convergent boundaries, as observed in the 2010-11 LLAP project, sustained by a buoyancy gradient (chapter 5 in Markowski and Richardson 2010). These boundaries may be found far from the lake's central axis, mainly due to the wind orientation and differences in solenoidal strength from opposite shores (Fig. 5). The boundaries are dynamic and may be distorted by horizontal shear instability (Steiger et al. 2012).

Convective and slantwise convective processes. LLAP snow bands may contain cells and lines that may be long-lived due to convective-scale processes. Processes that explain rotation in deep convective

storms also may apply to convection ~4 times more shallow. The combination of the local shear and stability profiles in LLAP bands may be sufficient to support convective cells with a rotating updraft similar to a supercell mesocyclone (Weisman and Klemp 1982; Weisman and Klemp 1984). For example, relatively shallow supercells (although not nearly as shallow as LLAP supercells) have been encountered in the highly sheared environment of hurricane rainbands (e.g., McCaul and Weisman 1996), despite the confinement of buoyancy to low-levels. It also is possible that rotation within LLAP bands may be the result of vortex sheet instability in which vertical vorticity is created and is subsequently enhanced at the leading edge of convergent (outflow) boundaries (e.g., Wakimoto and Wilson 1998; Lee and Wilhelmson 1997). LLAP storms often intensify more rapidly and persist longer than synoptic conditions would suggest due to a combination of lake-scale and convective-scale processes [based on the experience of T. Niziol and R. Hamilton, NWS forecasters in Buffalo, NY, and of Dr. Steiger in Oswego NY]. For example, LLAP bands have lasted several hours into a warm-air advection regime under a lowering capping inversion. Some bands may intensify due to the release of potential symmetric instability, given the presence of substantial albeit shallow baroclinicity. A large region of upright potential instability can be seen in Fig. 5 ($\frac{\partial \theta_e}{\partial z} < 0$). This region is surrounded by a region with a steep slope of the moist isentropes. Symmetric instability typically yields more stratiform precipitation (as in Fig. 3), whereas upright instability yields convective precipitation; the two instabilities may co-exist and slantwise ascent may release (upright) potential instability.

Lake-to-lake interactions: The proximity of the Laurentian Great Lakes supports lake-effect storm interactions. In some cases radar imagery reveals continuous snow bands from one lake to the next. In other cases less apparent connections exist, as residual moisture, heat, and circulation fields are carried across to affect snow bands over a downwind lake (Rodriguez et al. 2007). Under prevailing westerly flow, Lake Ontario is the farthest downwind. Hence, the heat and moisture fluxes from upwind lakes can significantly modify the atmosphere near and over Lake Ontario. Almost every intense cold-air outbreak with northwesterly flow produces a snow band between Lakes Huron and Ontario (Rodriguez et al. 2007). WRF simulations can capture this interaction (Ballentine and Zaff 2007), although with significant (>~10 km) errors in the location of these bands. Lake-to-lake connections are present in most intense LLAP events over the Eastern Great Lakes (e.g., Lake Storm 'Locust', which produced 3.5 m of snow in Redfield, NY in February 2007; NWS Buffalo 2009b).

1.3.3 *Precipitation growth and electrification processes*

Although dendrites and aggregates appear to dominate within LeS (Braham 1990), a variety of hydrometeor types may occur. Rimed particles and graupel are common in deep LeS-type bands in Japan (Maekawa et al. 1993; Kitagawa and Michimoto 1994). It is quite remarkable that LLAP LeS can produce lightning with cloud tops below 4 km. Some 4 to 6 LeS thunderstorm events with cloud-to-ground (CG) lightning occur annually over the Eastern Great Lakes (Moore and Orville 1990; Steiger et al. 2009; Letcher and Steiger 2010). The vast majority of the lightning occurs at the eastern end of both lakes, downwind of the longest fetch. These frequency estimates are based on National Lightning Detection Network (NLDN; Cummins et al. 2006) data, but spotter reports suggest there may be significantly more total lightning strikes, including cloud-to-cloud and intracloud lightning, which is rarely captured by the NLDN. For instance, in the 2 December 2005 LLAP storm, observers at SUNY-Oswego reported 20 flashes while the NLDN recorded only 5 flashes. They also reported heavy graupel precipitation during the periods of lightning.

The microphysics of surface-based cold-season electrically active shallow convection have been studied extensively using observations downwind of the Sea of Japan, where BL convection is often enhanced by orographic ascent (e.g., Michimoto 1991, 1993). Kitigawa and Michimoto (1994) found that the occurrence of lightning is heavily dependent on the altitude of the -10°C isotherm. They also examine the vertical distribution of electrical charge structures, something the OWLeS campaign is not equipped to do, with a single ground-based electric field mill (Section 1.5.3). But OWLeS is well-equipped to study the cloud microphysical processes leading to lightning.

Graupel plays a crucial role in vertically separating electrical charges through frictional collisions with smaller ice crystals and supercooled water droplets (Reynolds et al. 1957; Takahashi 1978). One of the most accepted hypotheses involves non-inductive (i.e., without background electric field) charge separation in which small ice crystals become positively charged and ascend to cloud top, while graupel particles become negatively charged and fall out (MacGorman and Rust 1998, pp. 61-75). Current electrification models strongly support the importance of graupel production in the -10 to -20°C layer (Zajac and Weaver 2002).

Steiger et al. (2009) found that the height of the storm equilibrium level (EL) relative to the -10°C isotherm can discriminate between LeS with and without lightning: most lightning events occurred when the EL was at least 1 km above the -10°C isotherm, and when that isotherm was higher than 1 km AGL.

1.4 Dual-polarization radar hydrometeor type classification and QPE of lake-effect snowfall

Dual-pol radar variables, combined with equivalent reflectivity factor (Z), have been shown to enable hydrometeor particle type identification (Zrnicek and Ryzhkov 1999; Vivekanandan et al. 1999) and to improve estimates of surface precipitation compared to estimates based on Z alone (Zrnicek and Ryzhkov 1996; Ryzhkov et al. 2005; Chandrasekar et al. 2008). The main dual-pol variables are differential reflectivity (Z_{DR}), specific differential propagation phase (K_{DP}), and the cross-correlation coefficient between horizontally and vertically polarized returns (ρ_{hv}). Since these variables are remarkably independent and poorly correlated (e.g., Gill et al. 2012), they contain far more information about hydrometeor shapes, habits, and density than Z alone. In dynamic systems such as LeS, precipitation processes are diverse and transient. Changes in time (e.g., from one DOW scan to the next) may be indications of processes such as hydrometeor sorting, melting/evaporation, or wet/dry growth by riming (Moisseev et al. 2012). The riming process is especially relevant to understand electrification of these systems. Cloud-resolving simulations of LeS, using both operational and experimental microphysics schemes, have yielded a diversity of vertical distributions and concentrations of cloud liquid water, graupel, and snow within these storms (Maesaka et al. 2006; Grecu and Olson 2008; Shi et al. 2010). Since combined dual-pol radar and *in situ* microphysical observations in winter storms are scarce (e.g., Liu and Chandrasekar 2000), and to our knowledge absent within LeS bands, little is known about hydrometeor diversity and distribution in LeS.

C-band dual-pol radar data have been collected in “sea-effect” snow bands near the NW coast of Japan (e.g., Fukao et al. 1991). Maekawa et al. (1993) inferred significant graupel concentrations in these bands by using a simple hydrometeor classification scheme based on graupel having low Z_{DR} and high Z (> 30 dBZ) values. Boodoo et al. (2012a) explored dual-pol values in a few LeS events, and Boodoo et al. (2012b) found dual-pol-identified graupel regions near lightning events in a LeS over Lake Huron and Ontario, using the C-band WKR radar in Ontario (see **Fig. 8** for WKR location). The advantages of dual-pol radar data for cloud microphysics research and QPE in LeS snowfall are promising but remain largely unexplored.

The S-band WSR-88D radars located within the OWLeS domain recently have been dual-pol upgraded. The WSR-88D hydrometeor classification algorithm (HCA) uses five dual-pol variables: Z_{DR} , K_{DP} , ρ_{hv} , and two texture parameters (Park et al. 2009). The HCA discriminates between 8 non-biotic classes: wet snow, dry aggregated snow, ice crystals with various orientations, graupel, hail/rain mixture, light/moderate rain, heavy rain, and “big drops” (Park et al. 2009). This classification then is used for improved QPE based on empirical relationships between rainrate and Z , Z_{DR} & K_{DP} (Giangrande and Ryzhkov 2008). The hydrometeor classification and QPE algorithms have been tested mainly in deep convective systems (Ryzhkov et al. 2005; Giangrande and Ryzhkov 2008; Park et al. 2009). The HCA was originally developed for warm-season weather (Istok et al. 2009) and has not been validated using *in situ* flight-level data in LeS. *The proposed OWLeS airborne and ground-based measurements and the recent dual-pol upgrade of the WSR-88D radars around Lake Ontario represent a unique, cost-effective opportunity to pursue the topics of dual-pol hydrometeor type classification validation (primarily) and QPE assessment (secondarily) in lake-effect precipitation systems, as well as deeper frontal systems of opportunity.*

Aside from the validation of HCA and QPE algorithms for the WSR-88D network, OWLeS aims to explore the microphysical processes in LeS through the examination of dual-pol fields using both operational S-band radars and deployable X-band radars (DOWs). The DOWs have the advantage of mobility, fine-spatial resolution and ability to observe low-level regions out of reach of the S-band radars. Several X-band hydrometeor classification algorithms (Snyder et al. 2010; Kouketsu and Uyeda 2010; Moreau et al. 2012) and QPE retrievals (e.g., Anagnostou et al. 2004; Anagnostou et al. 2006; Wang and Chandrasekar 2010) have been developed, with limited field evaluation. The simultaneous collection of dual-pol data at X- and S-bands, comprehensive profiler measurements, and *in situ* microphysical data during OWLeS affords the unique opportunity to study LeS microphysics and to validate and improve HCA and QPE algorithms.

1.5 Key OWLeS instrument platforms

One of the great strengths of OWLeS is the unprecedented resolution with which LeS bands will be

captured. OWLeS' main assets are: three mobile radars, an airborne radar and lidar, and an integrated profiling system, operating in the context of a dense surface network.

1.5.1 Center for Severe Weather Research (CSWR) Dual-Polarization and Rapid-Scan DOW radars

Three X-band mobile radars (DOWs) will be operated (<http://cswr.org/contents/aboutdows.php>). Two of the DOWs (DOW6 and DOW7) are dual-polarization, dual-frequency systems, which simultaneously permit fast scan rates (50° s^{-1}) and collection of the full suite of dual-polarimetric measurements (Z_{DR} , LDR , K_{DP} , and ρ_{hv}). Full time series data are collected, allowing for increased flexibility in post-processing the data. The third DOW, the Rapid Scan DOW (RSDOW), is a passive phased-array radar capable of collecting 6 levels of data simultaneously, which results in volumetric data every 10-20 s. Fine-scale spatial resolution is achieved with a 0.9° beamwidth, and 60 m (DOW6, DOW7) to 50 m (RSDOW) gates. All three radars employ staggered PRTs, resulting in large Nyquist velocities. The DOWs can collect data in PPI, RHI, and vertically pointing modes. Each DOW carries a telescoping boom measuring wind and state variables.

1.5.2 University of Wyoming King Air (UWKA) with radar and lidar

The UWKA (<http://flights.uwyo.edu/n2uw/>) contains a suite of atmospheric measurement probes, including eddy correlation flux measurements, a new high-precision positioning system [allowing very precise radar beam pointing angle determination and pressure perturbation estimation, Parish et al. (2007)], an aerosol size distribution probe (PCASP), new cloud microphysical probes such as the Cloud Imaging Probe and the Cloud Droplet Probe with ice shattering avoidance tip. It also carries two profiling remote sensors, a 95 GHz (3 mm) Doppler radar (the Wyoming Cloud Radar, WCR) and an eyesafe (355 nm) incoherent elastic polarization backscatter lidar (the Wyoming Cloud Lidar, WCL). The fine 2D resolution (10-30 m) of the WCR has contributed to several breakthroughs in the past decade, in our understanding of frontal systems, shallow convection, orographic precipitation and BL dynamics. The WCR will be operated with 5 fixed antenna positions. Three antenna combinations will be used (**Fig. 6**): (a) the nadir & slant-down (30° forward from nadir) antennas allows the dual-Doppler synthesis of the along-track 2D flow below the aircraft (Damiani and Haimov 2006); (b) the nadir & zenith antennas yield a vertical profile of fine-scale (~ 30 m resolution) reflectivity and Doppler velocity data, in which context *in situ* measurements can be interpreted; (c) single and dual-Doppler WCR data will also be collected to the right of the aircraft, using the side and slant-side antennas. Four antennas can be operated simultaneously. The zenith/side antenna can point in either direction, depending on the position of a mirror.

The WCL can also be used in profiling mode (above and below the aircraft) (Wang et al. 2012). The WCL detects aerosol layers, clouds, and precipitation. Liquid water cloud edges rapidly attenuate the lidar signal. The lidar depolarization ratio can be used to discriminate snow crystals. The LeS cloud top can be determined by WCR (looking up or down, depending on flight level) and WCL (looking down only). The WCL is expected to be able to capture the very first, very shallow streamers of lake-effect clouds near the upwind shore (e.g., Mayor and Eloranta 2001). In some regions the combination of WCR and WCL data may allow quantitative assessment of liquid and ice water content (e.g. Heymsfield et al. 2008; Wang et al. 2012).

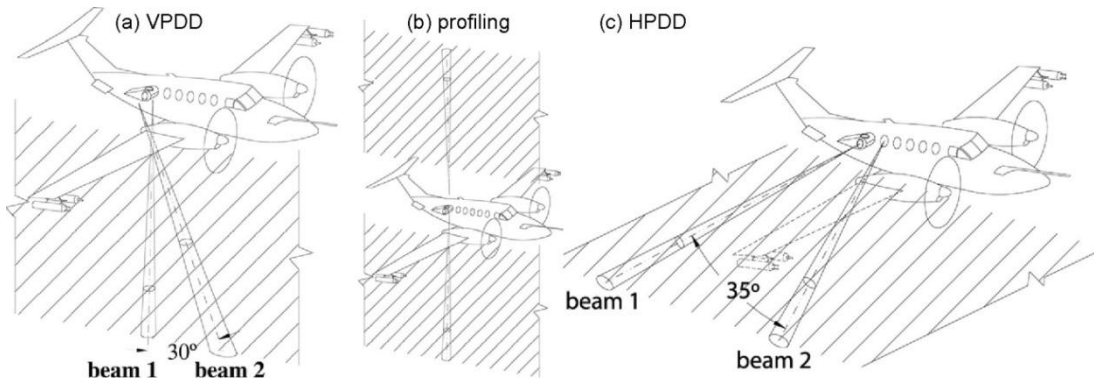


Fig. 6: WCR antenna options aboard the UWKA (from Damiani et al. 2006). The acronym VPDD (HPDD) refers to vertical (horizontal) plane dual-Doppler.

Yang and Geerts (2006) used vertical-plane and horizontal-plane WCR reflectivity and Doppler velocity observations to study the structure and dynamic forcing of coherent circulations in LeS over Lake Michigan in

an UWKA-only campaign in 2004. In the example in **Fig. 7**, the nadir and slant-forward Doppler velocities are synthesized on a vertical-plane grid with a resolution of $100 \times 100 \text{ m}^2$. Updrafts tend to coincide with higher radar reflectivity values, suggesting that the vertical drafts are somewhat persistent. In the presence of coherent circulations as seen in Fig. 7, the flight-level buoyancy, vertical velocity, vertically-integrated radar reflectivity, droplet concentration and snow crystal concentration all correlated positively, suggesting that the circulation is relatively long-lived, consistent with radar reflectivity animations. In other cases the correlations were much weaker, indicative of short-lived convective cells. Yang and Geerts (2006) found it difficult to detect the secondary circulation amidst the strong convective motions on most cross-band flight legs – Fig. 7 is one of the better examples of HCRs.

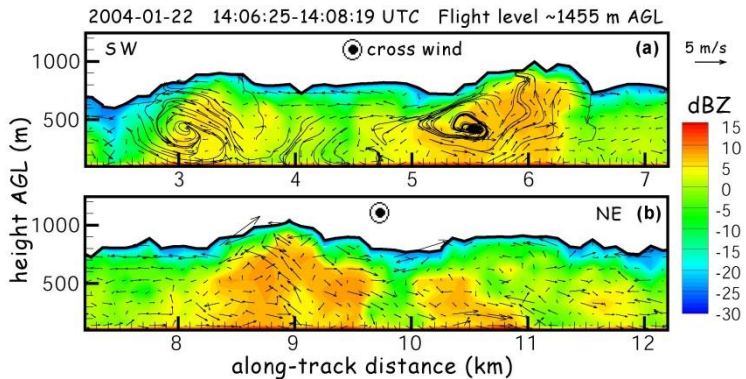


Fig. 7: Sample cross-section of vertical-plane WCR reflectivity and winds inferred from VPDD, for a UWKA flight track normal to the prevailing wind over Lake Michigan. The section is continuous but is cut in two panels (a and b) to maintain a 1:1 aspect ratio. The estimated fallspeed of snow (1.3 m s^{-1}) has been removed. The lines with arrows in (a) are select streamlines, tangential to the vectors. (from Yang and Geerts 2006)

1.5.3 Mobile Integrated Profiling System (MIPS)

The MIPS (<http://vortex.nsstc.uah.edu/mips/system/>) consists of a large van connected to a 24 ft trailer serving as the instrument platform. The MIPS configuration for the OWLeS field campaign will consist of the following instruments and corresponding measurement capabilities:

Remote sensing instruments:

- a 915 MHz Doppler wind profiler, providing mean horizontal wind at 15-30 min time intervals and Doppler spectra and spectral moments at vertical incidence at 1 min intervals.
- an X-band Profiling Radar (XPR), providing moments of the Doppler spectrum (reflectivity factor; Doppler velocity, i.e. hydrometeor vertical velocity; and spectral width) at 6 Hz and 60 m gate space, starting at $\sim 60 \text{ m AGL}$.
- a 12-channel Microwave Profiling Radiometer (MPR), providing vertical profiles of temperature, water vapor density, & cloud liquid water, and integrated water vapor & cloud water at 1 min intervals.
- a Vaisala CL-51 ceilometer, providing cloud base height and backscatter profile below cloud every 6 s at a vertical resolution of 10 m.
- an eye-safe Doppler wind Lidar with a 20 m resolution, scanning in RHI or PPI volume scanning modes.

Surface instrumentation:

- All meteorological variables at 1 Hz frequency, on a tower up to 10 m high.
- TPS-3100 Hot Plate precip gage (liquid water equivalent snow rate, Rasmussen et al. 2009, 2012)
- Parsivel disdrometer (particle size distribution)
- Electric field mill (vertical electric field)
- NCAR's Snowflake Video Imager (60 Hz; resolution 0.1 mm: snow size distribution and particle classification; Newman et al. 2009)

2. Objectives and hypotheses

This proposal has three related objectives (listed as objectives 4-6 in Section 1.1). The first two deal with fundamental BL and microphysical processes, while the third one is more applied. The following 11 specific hypotheses associated with these three objectives will be tested through the OWLeS field campaign and data analysis:

2.1 LLAP band intensification mechanisms (Section 1.3.2) Leads: Geerts, Steiger, Knupp

- LeS clouds can be detected first by lidar near the upwind shore, as steam fog becomes organized in streamers; generally some fetch over water is needed for the cloud bands to be detectable by

mm-wave radar; some may be seeded by ice crystals from residual LeS bands from an upstream lake, or by blowing snow, and thus be immediately apparent on radar.

- ii. Initially, near the upstream shore, multiple lidar-detectable bands may develop with a width that scales with the depth of the deepening CBL. The reduction to a single LLAP snow band, and the intensity and depth of that band, exceeding fetch-specific expectations, are mainly the result of solenoidally-driven currents arising from one or both wind-parallel lake shores.
- iii. The intensity of LLAP bands relates to upwind influences (e.g., humidity, stratification), surface heat fluxes over Lake Ontario, the strength and height of the stable layer, the temperature difference between the lake surface and the CBL top, and vertical wind shear.
- iv. LLAP bands contain one or more well-defined solenoidal boundaries with radar- and sounding-detectable low-level convergence and upper-level divergence; these boundaries may be distorted by lake-scale circulations and miso-vortices induced by horizontal shear along these boundaries.
- v. Some LLAP convective cells have a mesocyclone and separated up- and downdrafts, and dynamically behave as supercell storms.

2.2 LLAP band kinematics, microphysics and electrification (Section 1.3.3) *Leads: Kosiba/Wurman, Steiger, Frame*

- vi. LLAP bands have embedded buoyant cores yielding convective-scale updrafts, resulting in pockets of high liquid water and graupel concentrations.
- vii. Non-eddy resolving WRF simulations, even when run at high resolution, may significantly err in terms of LeS QPF, especially under strong wind, irrespective of the PBL or cloud microphysics scheme used. (Section 1.2, penultimate paragraph)
- viii. The X- and S-band dual-pol fields, combined with in situ measurements in the air and on the ground, yield new insights into the precipitation growth processes in LeS bands over the lake, as they move onshore, and over coastal terrain.
- ix. Lightning discharges in LLAP bands occur in regions of strong updrafts and high graupel concentrations, and mostly do not reach the ground.

2.3 Hydrometeor classification and QPE (Section 1.4) *Leads: Frame, Kosiba, Geerts*

- x. The operational WSR-88D dual-pol HCA accurately identify basic hydrometeor types in LeS, but can be refined. The OWLeS combined DOW and *in situ* datasets will improve experimental X-band HCAs.
- xi. The WSR-88D dual-pol snow rate estimation is superior to the Z-only snow rate estimation in LeS.

3. **Experimental design**¹

3.1 Mobile and fixed radars

The 3 DOWs will provide dual- and multiple-Doppler coverage (with baselines < 30 km) centered on the LLAP band (Fig. 8). Different scanning strategies will be employed for different meteorological conditions and research objectives. In general the RSDOW will be tasked with providing continuous low-level coverage in order to detail the evolution of rapidly evolving boundary layer structures, while the two dual-pol DOWs will complete deeper volumes in order to fully characterize the microphysical and kinematic properties of the LLAP bands. When the UWKA flies along the LLAP band (flight pattern #3, Section 3.2), then the centrally located dual-pol DOW will conduct RHIs along the band in the plane of MIPS and the WCR transect. This will provide unprecedented collocated information of hydrometeor type (dual-pol and *in situ*), as well as WCR vertical velocity, MIPS thermodynamic and radar profiling data, and the surface snow measurements. The DOW network (and MIPS) are adaptable during intensive operation periods (IOPs): their location at any of a set of pre-selected sites will be configured based on weather and the other OWLeS surface assets. After the field phase, radar data will be interpolated to a Cartesian grid using a two-pass Barnes scheme (Majcen et al. 2008) and then synthesized into 2D or 3D wind fields for kinematic analysis.

Aside from the DOWs, the most relevant WSR-88D radar is KTYX on top of the Tug Hill plateau (Fig. 8). Because of its elevation (the antenna is 460 m above Lake Ontario) and its upward look (lowest elevation angle is 0.5°) it cannot capture low-level phenomena over Lake Ontario. The NWS has considered a 0.2°

¹ More details on the experimental design of the entire OWLeS campaign can be found in the NSF LAOF request or at <http://www.atmos.uwyo.edu/~geerts/owles/>

base elevation and even negative angles for KTYX (Brown et al. 2007). If the LLAP band center axis makes landfall north of Oswego, at least one of the DOWs will be close enough to KTYX for multiple-Doppler synthesis. Occasionally LLAP bands form under ENE surface winds, making landfall between ROC and YHM (Fig. 8) (Spinar and Kristovich 2007). In that case KBUF (Buffalo NY) will be the target WSR-88D radar, and the OWLeS armada will be deployed between ROC and YHM. KBUF will be the target radar also on the rare occasion that a LLAP band forms over Lake Erie and not Lake Ontario.

3.2 UWKA flight patterns

Four types of flight patterns will be conducted (Fig. 8):

1. a low-level flux leg over open water in the vicinity of the main snow band, in order to determine surface heat fluxes, the lake surface IR temperature, the lidar cloud base height, and lake ice extent;
2. a series of cross-LLAP-band legs from the upwind cloud band formation region to the coast and (if the wind direction is right) over the Tug Hill Plateau, at two levels (the lowest safe flight level and just below cloud top, **Fig. 9**), in order to measure, at different points in the band's evolution, cloud and precip particles (phase, mass, size distribution, habit, riming amount), buoyancy, perturbation pressure, radar and lidar data in vertical transects, and the secondary circulation from WCR dual-Doppler synthesis;
3. an along-LLAP-band leg at mid-levels, in the vertical plane of a dual-pol DOW RHI and MIPS, to be flown repeatedly between geographically fixed points, in order to measure the same as above, esp. the *in situ* hydrometeor properties plus the WCR HPDD wind field to the right of the aircraft (Fig. 6c) (This leg will be attempted only if pattern #2 indicates that there is not too much airframe icing.);
4. spiral profiles offshore and possibly onshore over the depth of the LLAP band (Fig. 9), in order to document the hydrometeor and liquid water profiles (to be compared with the MIPS X-band and radiometer-derived profiles), and the secondary circulation and its thermodynamic forcing.

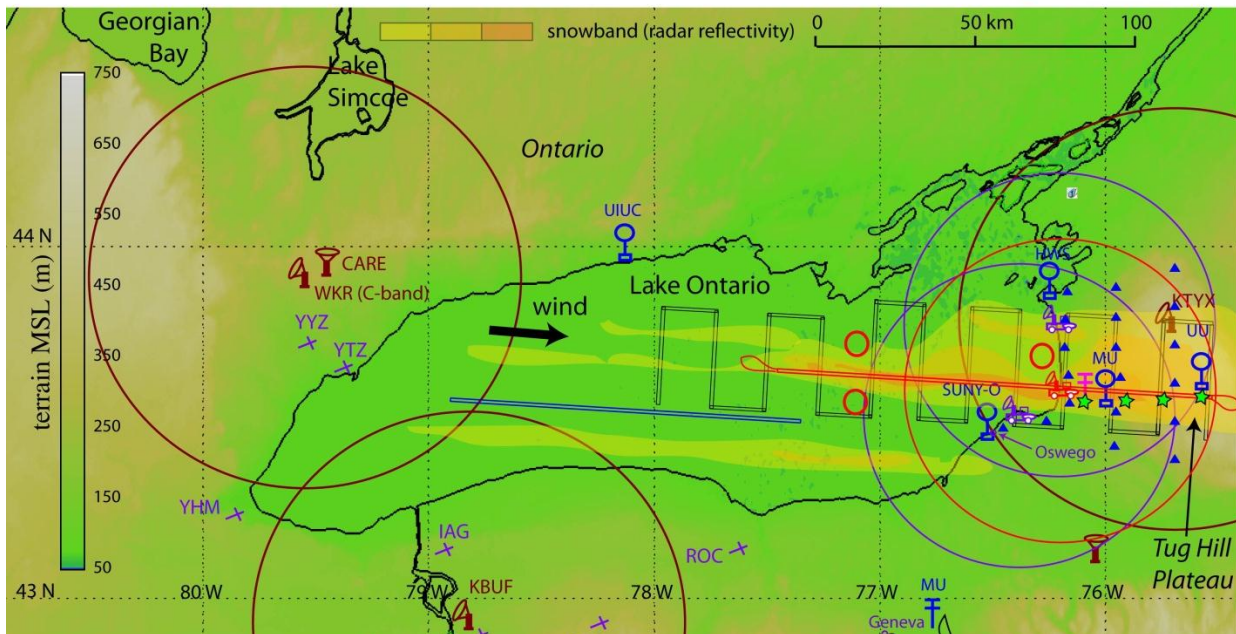
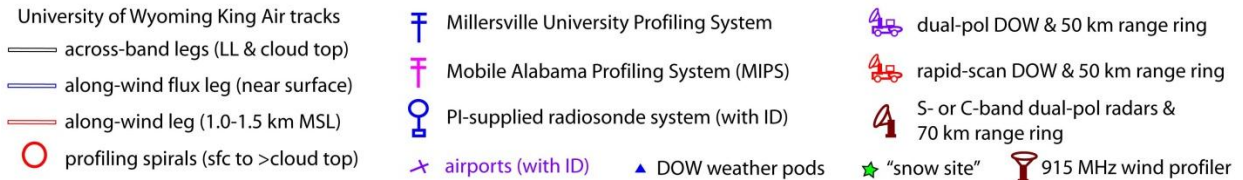


Fig. 8: Map showing Lake Ontario and surrounding terrain, schematic UWKA flight patterns, 3 DOWs, 5 mobile soundings, MIPS, and a network of DOW weather pods. The target snow bands are oriented with the mean wind, which is from the west for the lake-parallel snow band (shown schematically). The 70 km circles indicate the approximate range of radar coverage (0.5° elevation angle) for targets up to ~1000 m above the radar site. Good volume coverage is available within the 50 km circles drawn around the DOWs.

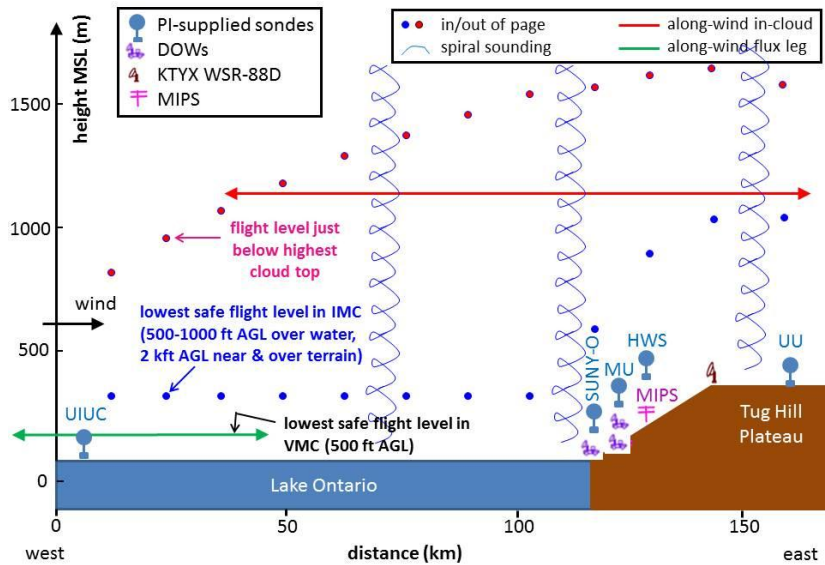


Fig. 9: Schematic vertical transect aligned with the mean low-level wind from the left (westerly to northwesterly flow). The blue and red dots indicate low-level and upper-level flight tracks in or out of the page and correspond with the black flight track in Fig. 8. The spirals indicate UWKA soundings.

Much of the flight time will be within the volume covered by KTYX and the DOW radars at rather close range (Fig. 8). For particle type validation purposes, the *in situ* particle probe data will be compared to X- and S-band dual pol data following the method by Nesbitt (2012). The geolocation uncertainty of the aircraft (~1 m) and radar gates (~500 m) (Vali and Rodi 2005) is smaller than the flight distance needed for the CIP and 2D-P to sample enough of the larger hydrometeors for this purpose. At a lower priority, similar flight patterns will be flown in pursuit of non-LeS precipitation systems of opportunity, especially deeper and warmer systems, in order to capture most or all WSR-88D hydrometeor types, and also to validate the melting layer algorithm (Giangrande et al. 2008).

3.3 Soundings, MIPS, and precipitation measurements

PI-provided rawinsondes will be released at 1-2 hour intervals during LLAP band events from 5 different locations (Fig. 8): the upwind shore (to examine upwind stratification & wind), the downwind shore on both sides of the LLAP band (to determine cross-band baroclinicity) and within the LLAP band (to determine band buoyancy), and over the Tug Hill Plateau (mainly in support of the OWLeS orography proposal). Key objectives are to quantify low-level air mass modification, fine vertical structure of shear and static stability, inversion height and strength, presence of and conditions for electrification, the lake-scale secondary circulation and its forcing, and orographic modification.

The MIPS will be located under the landfalling LLAP band, in the plane of the dual-pol DOW RHI, in order to document changes in shear and stability, cloud depth, vertical structure of liquid water, X-band reflectivity and vertical particle velocity ($W=w+V_T$), 915 MHz SNR, W, Doppler spectra, vertical electric field variations, and snowfall characteristics on the ground using the instruments listed in Section 1.5.3. Its mobility matches that of the DOWs, and MIPS will be moving with the DOWs as winds and LLAP band position shift during an IOP. Dedicated student teams will deploy and service up to ~20 CSWR weather pods in each IOP (Fig. 8). These pods measure T, RH, and wind direction/speed at 1 Hz frequency 1 m above the surface for up to 17 hours.

A transect of 4 “snow sites” from the east shore of Lake Ontario to the Tug Hill Plateau (Fig. 8) will document LLAP band precipitation characteristics. All snow sites will measure 1 Hz state variables, and trained students will photograph snow using high-resolution cameras mounted on a home-made stand above a rotating black velvet surface, and manually classify hydrometeors in terms of the 8 classes in the level III WSR-88D dual-pol algorithm (Section 1.4). These students will also regularly estimate fresh snow depth and density using a snow board and scale. And they will record the occurrence of lightning and/or thunder which will complement reports from the NWS spotter network around Lake Ontario.

Of the 4 snow sites, the coastal site is a supersite, including MIPS (Section 1.5.3), MU rawinsondes, and UU sheltered ETI gauge, and ultrasonic snow depth sensor. The 4th site, on Tug Hill, also is enhanced, with UU rawinsondes, ETI gauge, and ultrasonic snow depth sensor, and a UW Hotplate.

Several operational cumulative precipitation networks exist at time resolutions of 1 hour or worse. The CoCoRaHS precipitation network (www.cocorahs.org) is quite dense in the region of interest and its volunteers are trained to measure snow depth as well, from which bulk snow density can be estimated.

3.4 Field campaign timing and duration

The OWLeS field phase is scheduled for December-January, a time of the year when the Eastern Great Lakes region has been mostly ice-free in the last decade. Climatological studies based on visible satellite imagery suggest that LLAP snow bands are most likely between late October and late January (Kristovich and Steve 1995; Rodriguez et al. 2007; Steiger et al. 2009).

The duration of the field campaign (43 days) has been determined based on the climatological frequency of adequate cases. Climatological analyses have shown that the selected period typically yields about 11 LeS events, some lasting more than 1 day (Rodriguez et al. 2008). Of these, 3.2 tend to be LLAP events. Of these, a third (~1) can be expected to produce lightning (Letcher and Steiger 2010). A total of 7 LLAP events were observed during the 60 day LLAP project from mid-December to mid-February (Cermak et al. 2012b). LLAP events tend to last longer than short-fetch LeS events; most of them last more than 24 hours (see lake-effect page at <http://www.erh.noaa.gov/buff/>).

4. Relationship with the OWLeS-SAIL and OWLeS-orography proposals

The three key objectives of the OWLeS-SAIL collaborative proposal and the OWLeS-orography objective (Section 1.1) will be accomplished using the same facilities as part of the same field campaign (Section 1.5). The OWLeS-orography objective is best achieved under westerly flow impinging on the Tug Hill Plateau, thus it will primarily use the deployment depicted in Fig. 8. The OWLeS-SAIL objectives are best achieved under prevailing NW to W winds, for which the mobile facilities will be located near the southern shore of Lake Ontario and the Finger Lakes. The three proposals independently can be successful, but given the relative infrequency of LeS and the cost of mounting the field campaign, the proposed joint effort makes perfect sense. Moreover, there are numerous collaborations between us and the PIs on the two other proposals. This is not simply the result of data analysis expertise (Wurman/Kosiba- DOWs; Knupp-MIPS; Geerts – WCR ...), but also because of shared scientific interests (e.g., Kristovich – surface and BL processes in LLAP; Clark and Young – downwind persistence of LLAP bands; and vice versa, Kosiba – HCR circulations in regularly spaced LeS bands; Geerts – upstream influences on cloud band glaciation, orographic effects, and downwind persistence; Frame and Steiger – dual-pol signatures in non-LLAP snow bands; Steenburgh – coastal enhancement). The web of interactions is intricate and the separation of proposals is one of several possible organizations of a joint enterprise.

5. Tasks and schedule

The testing of our 11 hypotheses (Section 2) requires numerous specific tasks, listed in the Budget Justification for each of the 5 component proposals of the Collaborative Research. Most tasks are collaborative, with identified individual leads. These leads may be case-specific. For instance, Frame, Kosiba, Steiger, and Wurman each may lead the dual- and multiple Doppler analyses for one LLAP band event. These analyses will differ in their focus: in this example, Frame will relate the 3D flow field to the dual-pol variables (hypothesis 9), Kosiba will focus on fine-scale structures and their role in snow production (hypotheses 4, 5), Steiger will compare the kinematic and precipitation fields to Ballentine's WRF simulations (Section 6) and relate kinematic and dual-pol & *in situ* microphysics to lightning incidences (hypothesis 9). For these cases, Knupp and Kosiba will compare X- and S-band dual-pol variables in the context of MIPS profiles (hypothesis 10), and Geerts will validate the WSR-88D dual-pol particle ID and QPE algorithms with airborne *in situ* and ground-based measurements (hypotheses 10 and 11).

None of the hypotheses can be tested with a single instrument or platform. The LAOF request includes a Table (#2) listing the relative importance of the various facilities for the OWLeS hypotheses. For instance, hypothesis 10 requires at least one dual-pol DOW, the UWKA *in situ* probes and WCR, MIPS microphysics and sounding data, as well as manual snow characterizations.

Common activities for all OWLeS participants include:

Year 1: a planning meeting in upstate NY to develop the operations plan & preselect deployment sites, student training, the OWLeS field campaign itself, tentatively scheduled for 1-21 Dec 2013 and 3-24 Jan

2014, case prioritization discussion, and start of collaborative analyses;

Year 2: the 1st OWLeS Science Meeting (possibly at the site of an AMS meeting), the writing of an overview paper for the *Bull. Amer. Meteor. Soc.*; and

Year 3: the 2nd OWLeS Science Meeting, and continued collaborations on many papers, to be submitted mostly to *J. Atmos. Sci.* and *Mon. Wea. Rev.*

The OWLeS field campaign will serve as the basis for several other proposals under discussion amongst the present PIs and others, for instance to conduct large eddy simulations to study the validity of surface flux and microphysics parameterizations in non-eddy-resolving models. Both graduate and undergraduate students will be involved in all activities.

6. Educational initiatives

6.1 Training opportunities for OWLeS participants

The NSF LAOF Users Workshop held at NCAR in September 2007 highlighted the importance of the training of future observational scientists through participation in field work (Serafin et al. 2008). The OWLeS project uniquely responds to this need, not merely through graduate student involvement (mostly in post-field data analysis) customary in most NSF proposals. The OWLeS project will support a total of 35 student positions during the entire field phase. Most of these student participants (71%) are PI-supported, and ~3 out of 4 will be undergraduates from 4 participating universities (SUNY-Oswego, HWS, MU, and UIUC). Duties include rawinsonde preparation and release, pod deployment, DOW operations, MIPS and MUPS operations, UWKA flight, snow characterization, and forecasting / operations center support. Students will participate in campaign planning, instrument preparation, data collection, and analysis.

Forecasting support will be coordinated by Dr. Robert Ballentine at SUNY-Oswego. His team will be running WRF-ARW with an inner domain covering Lake Ontario and much of upstate New York at a 1 km resolution with at least 50 vertical levels favoring the PBL, using the best WRF physics choices (based on Ballentine's many years of experience). Students will be trained to help with the preparation of relevant forecast fields using Unidata-supported software (e.g. 850 mb T, RH, wind, surface wind and precipitation, skew T's), and with the analysis/interpretation of these fields. After the field phase, Ballentine will involve students in a sensitivity analysis of several microphysics, surface and BL parameterizations, and in an OWLeS sounding assimilation effort to examine the forecast impact of a mesoscale upper-air network.

While this massive student participation serves as a cost saving for both the deployment pool and proposals, the purpose primarily is educational. Students will be trained for their functions, will attend a winter survival and safety course, and will be monitored by the professional scientists and more experienced students. Students will be rotated once to enrich their experience. Through field participation, follow-up supervised data analysis, conference presentation (e.g. at the AMS annual meeting), and formal publication, undergraduates from SUNY-Oswego, HWS, MU and UIUC will fulfill their for-credit capstone research requirements. PIs from the three participating universities without graduate meteorology programs (Clark, Laird, Metz, Sikora, and Steiger) have a strong record of successful undergraduate research, and they have become personal magnets for their growing undergraduate programs in atmospheric sciences.

OWLeS will take advantage of non-IOP days between cold-air outbreaks. A 400-level (or cross-listed 400-500) 1-credit *OWLeS seminar series* will be organized, both on the science (microphysics and radar polarimetry, BL and mesoscale dynamics of LeS, orographic processes...) and on field instrumentation (ground-based remote sensing – active and passive; airborne and ground-based flux measurements; Doppler radar...). This will include visits to the facilities. Students will register at their home institutions and meet at the operations center auditorium. Local students not participating in OWLeS may enroll. The seminar sequence will be determined in advance; the exact timing depends on the IOP sequence. One seminar will be dedicated to the planning of an IOP, whereby select students decide on the UWKA flight plan, the schedule of rawinsonde releases, the DOW scan strategy and the deployment of participants in the field. This seminar, aimed at both graduate and undergraduate students, will be modeled after the seminar held as part of RICO (Rauber et al. 2007). The richness and breadth of instrumentation deployed in OWLeS will ensure that students participating in the seminar will be exposed to in-situ ground-based and airborne platforms and remote observing facilities, with sensors operating at several different frequencies, capturing multiple spatial scales, with each sensor dedicated to a specific measurement while serving as a component of a coordinated project-scale observing system.

6.2 Outreach

Several other universities in the vicinity offer undergraduate degree programs in meteorology or related fields (SUNY Brockport, Cornell, Penn State ...). We plan to arrange events for students from these schools as well as from the participating schools in the region (HWS, SUNY-Oswego) to visit the UWKA, the DOWs, MIPS and MUPS, all convening at the proposed UWKA's base airport (labeled PEO in Fig. 8). We plan to release and track a weather balloon with the visitors. Finally, we will develop a web-based (incl. Twitter and Facebook) OWLeS Outreach Program similar to the program at MU where teachers from local high schools, community colleges, and universities can request an on-site visit to the facilities.

7. Results from prior NSF support

7.1 **Steiger and Frame:** AGS-0724318, Collaborative Research: Dual-Polarimetric Doppler-on-Wheels Observations of Long Lake-Axis-Parallel Lake-effect Storms over Lakes Erie and Ontario, \$86,761 (Steiger) and \$34,711 (Frame), 9/1/2010 – 8/31/2012.

Seven lake-effect events were sampled by a DOW between 12/15/2010 and 2/11/2011 over and downwind of Lake Ontario as part of the EAGER-funded LLAP campaign. Some key features of the intense long-fetch snow bands revealed by the DOW data include miso-vortices, bounded weak echo regions, and jets (Steiger et al. 2012). The majority of the manually analyzed vortices had diameters less than 1 km, as in Fig. 1a. The fine detail provided by the DOW shows multiple convergent boundaries at various locations within these intense LLAP bands. Vortices formed along these boundaries, probably as a result of horizontal shear instability. Animations of these boundaries suggest that they were convectively generated as they moved away from the reflectivity core. In at least one instance the boundary formed an intense secondary band of convection. SUNY-Oswego undergraduate students Keith Jaszka, Tim Kress, Brett Rathbun, Daniel Ruth, and Robert Schrom are co-authors Steiger et al. (2012). Dr. Steiger presented initial findings at the 2011 AMS Radar Conference and Daniel Ruth presented this work at the 2012 AMS Annual Meeting.

Ahasic et al. (2012) and Cermak et al. (2012a) show that the Z_{DR} in embedded convective cells, with snow pellets and even graupel observed on the ground, tends to be higher than in the ambient more stratiform LLAP band, where dry aggregates usually dominate, even after neutralization of the effects of reflectivity and attenuation. This is consistent with some previous studies (e.g., Hall et al 1984; Straka et al. 2000), and is attributed to a preferred fall orientation of snow pellets not observed for aggregates. Also consistent with previous work is the positive correlation found in lake-effect snow between K_{DP} and $Z_{\rho_{hv}}$ values are highest for dendritic snowflakes, and lowest for mixtures of pellets and dendrites. This makes sense because ρ_{hv} is greatest when scatterers are in a single phase (both liquid water and ice crystals are required for snow pellet formation). The dual-pol signatures of the hook echoes surrounding most misovortices (Steiger et al. 2012) were generally indistinguishable from the surrounding banded or cellular echoes, suggesting that hydrometeors in these features are rapidly advected into the miso-circulation. Yet in a 10 km diameter mesovortex a Z_{DR} maximum was found on its perimeter, in particular in the convective cells that punctuated this perimeter. UIUC undergraduates Ahasic and Cermak were involved in this research for 2-4 semesters and gave oral presentations at the 2012 AMS Annual Meeting. They are first and second authors on Ahasic et al. (2012). Both have enrolled in graduate programs in atmospheric sciences starting in Fall 2012, with plans to obtain a PhD.

7.2 **Knupp:** AGS-0833995, Collaborative Research: Mesoscale and Microscale Processes in Extratropical Cyclones. 1/1/09-12/31/12, \$416K. In collaborative research with the UIUC, Knupp participated in the Profiling of Winter Storms (PLOWs) field campaign, which targeted the trowal region of cyclones over the Midwest (Rauber et al. 2012) during 2008-2009. The PLOWs campaign used the WCR and cloud lidar on the NCAR C-130; the MIPS and Mobile Alabama X-band dual pol radar, soundings, and WRF simulations to demonstrate that elevated upright convection is ubiquitous across the comma head of many continental winter cyclones. The UAH research efforts are focusing on the 10 January 2009 cyclone (northern Alabama) with associated convective snow and lightning. The periodic enhancement in SNR, vertical motion, and spectrum width in the MIPS 915 MHz profiler data suggests gravity wave passages over the MIPS, with corresponding enhancements in supercooled cloud water and formation of large aggregates via riming and aggregation. Kelvin-Helmholtz waves were also evident along and above the 4 km AGL level in RHI scans over the MIPS location from MAX and C-band ARMOR dual pol radars. Dual-Doppler retrievals

from ARMOR and KHTX 88D indicate undulations in the wind field associated with low-level wave features, as well as in the wind field at 4 km associated with the KH waves. Analysis of vertical velocity retrievals show linear couplets of upward and downward vertical velocities which is also indicative of wave passages in the precipitation shield of this event. Analysis of dual-polarimetric radar and North Alabama Lightning Mapping Array (NALMA) data indicate that lightning flashes during this winter weather event propagated upward from the ground (likely from transmission towers) and then horizontally 10's of kilometers within/below regions of distinct layering in the correlation coefficient (ρ_{hv}). NALMA data overlays indicate that lightning flash propagation primarily occurred between 0°C and -5°C in a water saturated environment, in which ρ_{hv} trended more toward horizontally oriented ice crystals and aggregates. Much of the analysis is being conducted by Ph.D. student Ryan Wade, who will participate in OWLeS. More information on this case and on PLOWS, is provided in Rauber et al. (2012) and Wade and Knupp (2012).

7.3 Kosiba and Wurman: With support from NSF-AGS-0801041 "Collaborative Research: VORTEX2: Multi-Scale and Multi-Platform Study of Tornadoes, Supercell Thunderstorms, and Their Environments", \$1,508,066, 06/2008-05/2013, and NSF-AGS-0910737 "Modeling and Analysis of the Landfalling Hurricane Boundary Layer", \$512,826, 09/2009-08/2013. The CSWR PI's Karen Kosiba and Josh Wurman have led or co-authored the following 20 peer-reviewed manuscripts, mostly published, some in review, others whose analysis is nearly complete and in final preparation for submission. The amount of effort supporting the work leading to these publications has varied from major to minor. In most cases, these are the results of multiple-Doppler and/or single-Doppler and/or GBVTD (ground-based velocity track display) analyses of radar and/or thermodynamic data, from VORTEX2 or prior experiments and from hurricane studies. Wurman (2010a, b); Wurman et al. (2010); Kosiba and Wurman (2010); Markowski et al. (2010); Marquis et al. (2011); Wakimoto et al. (2011); Potvin et al. (2011); Markowski et al. (2011); Chan et al. (2011); Atkins et al. (2012); Wakimoto et al. (2012); Markowski et al. (2012a,b); Kosiba et al. (2012); Wurman et al. (2012); Toth et al. (2012); Wurman et al. (2013); Kosiba et al. (2013); Alexander and Wurman (2013).

7.4 Geerts: ATM-0444254 "Dynamical Processes of Orographic Cumuli", \$460,473, 11/2005 – 4/2009 and AGS-0849225, "Dynamical Processes of Orographic Cumuli II", \$475,985, 10/2009- 9/2012 (<http://www.atmos.uwyo.edu/~geerts/cupido/>). The development of the CBL around a mountain, the interaction of orographic BL circulations with cumulus convection, and Cu dynamics have been our main topics of research following the CuPIDO (Cumulus Photogrammetric, In-situ and Doppler Observations) campaign in the summer of 2006 around the Santa Catalina Mountains in Arizona (Damiani et al. 2008). While the CuPIDO environment was vastly different, the campaign had some similarities with OWLeS: a localized heat source for Cu convection, mixed phase cloud dynamics, and some identical tools.

Geerts et al. (2008) developed a technique to compute horizontal perturbation pressure gradients from data collected at different elevations and demonstrate the diurnal cycle of solenoidal forcing that drives anabatic surface flow. Demko et al. (2009) examined the evolution of mountain-scale convergence, using data from both stations positioned around the mountain and UWKA data. They found some evidence for a toroidal heat-island circulation. The daytime evolution of the CBL and orographic circulation were studied further using WRF simulations that assimilate CuPIDO surface and sounding data in two papers: the evolution without deep convection appears in Demko and Geerts (2010a), and the interaction with deep convection is described in Demko and Geerts (2010b). Demko received his PhD in 2009. A 2nd PhD student, Yonggang Wang, authored 6 papers on Cu dynamics and defended in December 2011. Based on composite data in the exit region of cumulus clouds, Wang and Geerts (2009) proposed a correction for measured temperature (using a commonly used immersion sensor) in and near clouds. Wang and Geerts (2010) then improved the description of humidity variations near Cu by means of a new fast-response lyman- α humidity probe. These first two steps were needed because of the uncertainty in buoyancy estimation of buoyancy near clouds, due to uncertain humidity and temperature measurements in and near clouds. Wang et al. (2009) used the improved measurements to document buoyancy variations in and near Cu. With the new instruments and techniques, we are now in a position to estimate buoyancy across LeS bands more accurately than did Yang and Geerts (2006). Yonggang Wang then incorporated WCR with the *in situ* data, first to document Cu detrainment patterns (Wang and Geerts 2011), and then to describe the typical Cu cloud top vortex circulation using single-Doppler (Wang and Geerts 2012) and dual-Doppler data (Wang and Geerts 2013). A 3rd PhD student, Xin Zhou, is examining the relationship between soil moisture and the development of the CBL, the thermally-forced orographic circulation, convection, and precipitation, through two months of CuPIDO observations (Zhou and Geerts 2012) and WRF simulations (Zhou and Geerts 2013).

References

- Agee, E.M., and S.R. Gilbert, 1989: An aircraft investigation of mesoscale convection over Lake Michigan during the 10 January 1984 cold air outbreak. *J. Atmos. Sci.*, **46**, 1877-1897.
- Ahasic, E. T., J. W. Frame, and T. R. Cermak, 2012: Classification of precipitation types in lake-effect snow events using dual-polarimetric Doppler radar observations. Preprints, 16th Symposium on Meteorological Observation and Instrumentation, New Orleans, LA, Amer. Meteor. Soc.
- Alexander, C. and J. Wurman, 2013: A radar based climatology of tornadoes. To be submitted to *Mon. Wea. Rev.*
- Anagnostou, E. N., M. Grecu, M. N. Anagnostou, 2006: X-band polarimetric radar rainfall measurements in Keys Area Microphysics Project. *J. Atmos. Sci.*, **63**, 187-203.
- Anagnostou, E. N., M. N. Anagnostou, W. F. Krajewski, A. Kruger, and J. M. Benjamin, 2004: High-resolution rainfall estimation from X-band polarimetric radar measurements. *J. Hydrometeorol.*, **5**, 110-128.
- Atkins, N. T., A. McGee, R. Ducharme, R. M. Wakimoto, and J. Wurman, 2012: The LaGrange Tornado during VORTEX2. Part II: Photogrammetric Analysis of the Tornado Combined with Dual-Doppler Radar Data. *Mon. Wea. Rev.*, in press, <http://dx.doi.org/10.1175/MWR-D-11-00285.1>
- Ballentine, R. J., and D. Zaff, 2007: Improving the understanding and prediction of lake-effect snowstorms in the eastern Great Lakes region. Final Report to the COMET Outreach Program, Award No. S06-58395, 41 pp.
- Ballentine, R. J., A. J. Stamm, E. E. Chermack, G. P. Byrd and D. Schleede, 1998: Mesoscale model simulation of the 4-5 January 1995 lake-effect snowstorm. *Wea. Forecasting*, **13**, 893-920.
- Ballentine, R. J., and D. Zaff, 2007: Improving the understanding and prediction of lake-effect snowstorms in the eastern Great Lakes region. Final Report to the COMET Outreach Program, Award No. S06-58395, 41 pp.
- Bard, L., and D. A. R. Kristovich, 2012: Trend reversal in Lake Michigan contribution to snowfall. *J. Appl. Meteor. Climatol.* In press
- Braham, R. R., Jr., 1990: Snow particle size spectra in lake-effect snows. *J. Applied Meteor.*, **29**, 200-207.
- Braham, R. R., Jr., and M. J. Dungey, 1995: Lake-effect snowfall over Lake Michigan. *J. Applied Meteor.*, **34**, 1009-1019.
- Braham, R. R., and D.A.R. Kristovich, 1996: On calculating the buoyancy of cores in a convective boundary layer. *J. Atmos. Sci.*, **53**, 654-658.
- Brown, R. A., T. A. Niziol, N. R. Donaldson, P. I. Joe, and V. T. Wood, 2007: Improved detection using negative elevation angles for mountaintop WSR-88Ds. Part III: Simulations of shallow convective activity over and around Lake Ontario. *Wea. Forecasting*, **22**, 839-852.
- Boodoo, S., D. Hudak, V. N. Bringi, L. Bliven, G. J. Huang, N. Donaldson, and M. Leduc, 2012a: C-Band dual polarimetric observations of snow events in southern Canada. ERAD conference, Toulouse, France, 25-29 June. (oral)
- Boodoo, S., D. Hudak, N. Donaldson, M. Leduc, L. Bliven, 2012b: C-Band dual polarimetric observations of snow events with and without lightning over the Great Lakes region in southern Canada. ERAD conference, Toulouse, France, 25-29 June. (poster)
- Brown, L.C., and C.R. Duguay, 2010: The response and role of ice cover in lake-climate interactions. *Progress in Physical Geography*, **34**, 671-704. doi:10.1177/0309133310375653.

- Burnett, A. W., M. E. Kirby, H. T. Mullins, and W. P. Patterson, 2003: Increasing Great Lake-effect snowfall during the twentieth century: A regional response to global warming? *J. Climate*, **16**, 3535-3541.
- Byrd, G. P., R. A. Anstett, J. E. Heim and D. M. Usinski, 1991: Mobile sounding observations of lake-effect snowbands in western and central New York. *Mon. Wea. Rev.*, **119**, 2323-2332.
- Cermak, T, E. Ahasic, J. Frame, S. Steiger, J. Wurman, and K. Kosiba, 2012a: Dual-Polarization radar observations of long-lake-axis parallel lake-effect snow bands over Lake Ontario. To be submitted to *Mon. Wea. Rev.*
- Cermak, T. R., J. W. Frame, and E. T. Ahasic, 2012b: Dual-polarization observations of vortices and cellular convection within lake-effect snow bands. Preprints, 16th Symposium on Meteorological Observation and Instrumentation, New Orleans, LA, Amer. Meteor. Soc.
- Chan, P.W, J. Wurman, C.M. Shun, P. Robinson, and K. Kosiba, 2011: Application of a method for the automatic detection and GBVTD analysis of a tornado passing across the Hong Kong International Airport, *Atmos. Res.*, **106**, 18-29.
- Chandrasekar, V., A. Hou, E. Smith, V.N. Bringi, S.A. Rutledge, E. Gorgucci, W.A. Petersen, and G.S. Jackson, 2008: Potential role of dual- polarization radar in the validation of satellite precipitation measurements: rationale and opportunities. *Bull. Amer. Meteor. Soc.*, **89**, 1127-1145.
- Chang, S. S., and R. R. Braham, Jr., 1991: Observational study of a convective internal boundary layer over Lake Michigan. *J. Atmos. Sci.*, **48**, 2265-2279.
- Clark, T.L., T. Hauf, and J.P. Kuettnner, 1986: Convectively forced internal gravity waves: Results from two-dimensional numerical experiments. *Quart. J. Roy. Met. Soc.*, **112**, 899-925.
- Cooper, K.A., M.R. Hjelmfelt, R.G. Derickson, D.A.R. Kristovich, and N.F. Laird, 2000: Numerical simulation of transitions in boundary layer convective structures in a lake-effect snow event. *Mon. Wea. Rev.*, **128**, 3283-3295.
- Cummins, K. L., J. A. Cramer, C. J. Biagi, E. P. Krider, J. Jerauld, M. A. Uman, and V. A. Rakov, 2006: The U.S. National Lightning Detection Network: Post-upgrade status. Preprints, 2nd Conf. on Meteorological Applications of Lightning Data, Atlanta, GA, Amer. Meteor. Soc., CD-ROM, 6.1.
- Damiani R., and S. Haimov, 2006: A high-resolution dual-Doppler technique for fixed multi-antenna airborne radar. *IEEE Trans. Geosci. Remote Sens.*, **44**, 3475-3489.
- Damiani, R., G. Vali, and S. Haimov, 2006: The structure of thermals in cumulus from airborne dual-Doppler radar observations. *J. Atmos. Sci.*, **63**, 1432-1450.
- Damiani, R., and G. Vali, 2007: Evidence for tilted toroidal circulations in cumulus. *J. Atmos. Sci.*, **64**, 2045-2060.
- Damiani, R., J. Zehnder, B. Geerts, J. Demko, S. Haimov, J. Petti, G.S. Poulos, A. Razdan, J. Hu, M. Leuthold, and J. French, 2008: Cumulus Photogrammetric, In-situ and Doppler Observations: The CuPIDO 2006 Experiment. *Bull. Amer. Meteor. Soc.*, **89**, 57-73.
- Demko, J. C., B. Geerts, J. Zehnder, and Q. Miao, 2009: Boundary-layer energy transport and cumulus development over a heated mountain: an observational study. *Mon. Wea. Rev.*, **137**, 447-468.
- Demko, J. C., B. Geerts, J. Zehnder, and Q. Miao, 2009: Boundary-layer energy transport and cumulus development over a heated mountain: an observational study. *Mon. Wea. Rev.*, **137**, 447-468.
- Demko, J.C., and B. Geerts, 2010a: A numerical study of the evolving convective boundary layer and orographic circulation around the Santa Catalina Mountains in Arizona. Part I: Circulation without deep convection. *Mon. Wea. Rev.*, **138**, 1902-1922.

- Demko, J.C., and B. Geerts, 2010b: A numerical study of the evolution of the convective boundary layer and orographic circulations around the Santa Catalina Mountains in Arizona. Part II: Interaction with deep convection. *Mon. Wea. Rev.*, **138**, 3603-3622.
- Demoz, B., and Co-authors, 2006: Dryline on 22 May 2002 during IHOP: convective scale measurements at the profiling site. *Mon. Wea. Rev.*, **134**, 294-310.
- Drennan, W. M., J. A. Zhang, J. R. French, C. McCormick, and P. G. Black, 2007: Turbulent fluxes in the hurricane boundary layer. Part II: Latent heat flux. *J. Atmos. Sci.*, **64**, 1103-1115.
- Emanuel, K. A., 1986: An air-sea interaction theory for tropical cyclones. Part I: Steady-state maintenance. *J. Atmos. Sci.*, **43**, 585-604.
- Etling, D. and Brown, R.A., 1993: Roll vortices in the planetary boundary layer: a review. *Bound.-Layer Meteor.*, **65**, 215-248.
- Fukao, S., Y. Maekawa, Y. Sonoi, and F. Yoshino, 1991: Dual polarization radar observation of thunderclouds on the coast of the Sea of Japan in the winter season. *Geophys. Res. Lett.*, **18**, 179-182.
- Geerts, B., Q. Miao, and J.C. Demko, 2008: Pressure perturbations and upslope flow over a heated, isolated mountain. *Mon. Wea. Rev.*, **136**, 4272-4288.
- Giangrande, S.E., and A.V. Ryzhkov, 2008: Estimation of rainfall based on the results of polarimetric echo classification. *J. Appl. Meteor. Climatol.*, **47**, 2445-2462.
- Giangrande, S.E., J.M. Krause, and A.V. Ryzhkov, 2008: Automatic designation of the melting layer with a polarimetric prototype of the WSR-88D radar. *J. Appl. Meteor. Climatol.*, **47**, 1354-1364.
- Gill, R.S., M. B. Soerensen, T. Boevith, J. Koistinen, M. Peura, D. Michelson, R. Cremonini, 2012: BALTRAD dual polarization hydrometeor classifier. ERAD conference, Toulouse, France, 25-29 June. (oral)
- Greco, M., and W.S. Olson, 2008: Precipitating snow retrievals from combined airborne cloud radar and millimeter-wave radiometer observations. *J. Appl. Meteor. Climatol.*, **47**, 1634-1650.
- Hall, M., J. Goddard, and S. Cherry, 1984: Identification of hydrometeors and other targets by dual-polarization radar. *Radio Sci.*, **19**, 132-140.
- Heymsfield, A. J., et al., 2008: Testing and evaluation of ice water content retrieval methods using radar and ancillary measurements. *J. Appl. Meteor.*, **47**, 153-163.
- Hjelmfelt, M. R., 1990: Numerical study of the influence of environmental conditions on lake-effect snowstorms over Lake Michigan. *Mon. Wea. Rev.*, **118**, 138-150.
- Istok, M.J., and co-authors, 2009: WSR-88D dual polarization initial operational capabilities. 25th Conf. on International Interactive Information and Processing Systems (IIPS) for Meteorology, Oceanography, and Hydrology, AMS, Phoenix AZ, Jan 2009.
- Keighton, S., and Co-authors, 2009: A collaborative approach to study northwest flow snow in the Southern Appalachians. *Bull. Amer. Meteor. Soc.*, **90**, 979-991.
- Kelly, R. D., 1982: A single Doppler radar study of horizontal-roll convection in a lake-effect storm. *J. Atmos. Sci.*, **39**, 1521-1531.
- Kelly, R.D., 1984: Horizontal roll and boundary-layer interrelationships observed over Lake Michigan. *J. Atmos. Sci.*, **41**, 1816-1826.
- Kitigawa, N., and K. Michimoto, 1994: Meteorological and electrical aspects of winter thunderclouds. *J. Geophys. Res.*, **99**, 10713-10721.
- Kosiba, K., and J. Wurman, 2010: The three-dimensional axisymmetric wind field structure of the Spencer, South Dakota, 1998, tornado. *J. Atmos. Sci.*, **67**, 3074-3083.

- Kosiba, K. A., J. Wurman, Y. Richardson, P. Markowski, and P. Robinson, 2012: The genesis of the Goshen County, Wyoming, tornado (5 June 2009). Accepted to *Mon. Wea. Rev.*, pending revisions.
- Kosiba, K. A. J. Wurman, F. Masters, and P. Robinson, 2013: Mapping of the low-level winds in Hurricane Rita using fine-scale radar and anemometer data. To be submitted to *Wea. Forecasting*.
- Kouketsu, T. and H. Uyeda, 2010: Validation of hydrometeor classification method for X-band polarimetric radar comparison with ground observation of solid hydrometeor. *Proc. Sixth European Conference on Radar in Meteorology and Hydrology (ERAD2010)*.
- Kristovich, D.A.R., 1993: Mean circulations of boundary-layer rolls in lake-effect snow storms. *Bound.-Lay. Meteor.*, **63**, 293-315.
- Kristovich D. A. R., and R. A. Steve III, 1995: A satellite study of cloud-band frequencies over the Great Lakes. *J. Appl. Meteor.*, **34**, 2083-2090.
- Kristovich, D. A. R., and R. R. Braham, Jr., 1998: Profiles of moisture fluxes in snow-filled boundary layers. *Bound.-Lay. Meteor.*, **87**, 195-215.
- Kristovich, D.A.R., N.F. Laird, M.R. Hjelmfelt, R.G. Derickson, and K.A. Cooper, 1999: Transitions in boundary layer meso- γ convective structures: an observational case study. *Mon. Wea. Rev.*, **127**, 2895-2909.
- Kristovich, D.A.R., and Co-authors, 2000: The Lake—Induced Convection Experiment and the Snowband Dynamics Project. *Bull. Amer. Meteor. Soc.*, **81**, 519-542
- Kristovich, D.A.R., N.F. Laird, and M.R. Hjelmfelt, 2003: Convective evolution across Lake Michigan during a widespread lake-effect snow event. *Mon. Wea. Rev.*, **131**, 643-655.
- Kunkel K.E., N.E. Westcott NE, and D.A.R. Kristovich, 2002. Assessment of potential effects of climate change on heavy lake-effect snowstorms near Lake Erie. *Journal of Great Lakes Research*, **28**, 521-536.
- Kunkel, K. E., and co-authors, 2009: A New Look at Lake-Effect Snowfall Trends in the Laurentian Great Lakes Using a Temporally Homogeneous Data Set. *Journal of Great Lakes Research*, **35**, 23-29. doi: <http://dx.doi.org/10.1016/j.jglr.2008.11.003>
- Laird, N. F., J. E. Walsh, and D. A. R. Kristovich, 2003: Model simulations examining the relationship of lake-effect morphology to lake shape, wind direction, and wind speed. *Mon. Wea. Rev.*, **131**, 2102-2111.
- Lee, B. D., and R. B. Wilhelmson, 1997: The numerical simulation of non-supercell tornadogenesis. Part I: Initiation and evolution of pretornadic mesocyclone circulations along a dry outflow boundary. *J. Atmos. Sci.*, **54**, 32-60.
- Letcher, T., and S. M. Steiger, 2010: Lake-effect lightning climatology of the Great Lakes. *National Weather Digest*, **34**, 157-168.
- Liu, H., and V. Chandrasekar, 2000: Classification of hydrometeors based on polarimetric radar measurements: development of fuzzy logic and neuro-fuzzy systems, and in situ verification. *J. Atmos. Oceanic Technol.*, **17**, 140-164.
- MacGorman, D. R., and W. D. Rust, 1998: *The Electrical Nature of Storms*. Oxford University Press, 422 pp.
- McCaul, E. W., and M. L. Weisman, 1996: Simulations of shallow supercell storms in landfalling hurricane environments. *Mon. Wea. Rev.*, **124**, 408-429.
- Maesaka, T., G. W. K. Moore, Q. Liu, and K. Tsuboki, 2006: A simulation of a lake effect snowstorm with a cloud resolving numerical model. *Geophys. Res. Lett.*, **33**, L20813, doi:10.1029/2006GL026638

- Mann, G.E., R.B. Wagenmaker, and P.J. Sousounis, 2002: The influence of multiple lake interactions upon lake-effect storms. *Mon. Wea. Rev.*, **130**, 1510-1530.
- Markowski, P., M. Majcen, Y. Richardson, J. Wurman, 2011: Characteristics of the wind field in a trio of nontornadic low-level mesocyclones observed by the Doppler On Wheels radars", *E. Journal of Severe Storms Meteor.*, **6**, 1-48.
- Markowski, P., Y. Richardson, J. Marquis, J. Wurman, K. Kosiba, P. Robinson, D. Dowell, E. Rasmussen, and R. Davies-Jones, 2012a: The pretornadic phase of the Goshen County, Wyoming, supercell of 5 June 2009 intercepted by VORTEX2. Part I: Evolution of kinematic and surface thermodynamic fields. *Mon. Wea. Rev.*, in press, <http://dx.doi.org/10.1175/MWR-D-11-00336.1>.
- Markowski, P., Y. Richardson, J. Marquis, R. Davies-Jones, J. Wurman, K. Kosiba, P. Robinson and E. Rasmussen, 2012b: The pretornadic phase of the Goshen County, Wyoming, supercell of 5 June 2009 intercepted by VORTEX2. Part II: Lagrangian circulation analysis. *Mon. Wea. Rev.*, in press, <http://dx.doi.org/10.1175/MWR-D-11-00337.1>.
- Marquis, J., Y. Richardson, P. Markowski, D. Dowell, J. Wurman, 2011: The maintenance of tornadoes observed with high-resolution mobile Doppler radars, *Mon. Wea. Rev.*, **139**, 5017-5043.
- Mayor, S.D., and E.W. Eloranta, 2001: Two-dimensional vector wind fields from volume imaging lidar data. *J. Appl. Meteor.*, **40**, 1331-1346.
- Maekawa, Y., S. Fukao, Y. Sonoi, and F. Yoshino, 1993: Distribution of ice particles in wintertime thunderclouds detected by a C band dual polarization radar: A case study. *J. Geophys. Res.*, **98**, 16,613-16,622.
- Majcen, M., P. Markowski, Y. Richardson, D. Dowell, and J. Wurman, 2008: Multi-pass objective analyses of radar data. *J. Atmos. Oceanic Tech.*, **25**, 1845-1858.
- Miao, Q., B. Geerts, and M. LeMone, 2006: Vertical velocity and buoyancy characteristics of coherent echo plumes in the convective boundary layer, detected by a profiling airborne radar. *J. Appl. Meteor. Climat.*, **45**, 838-855.
- Miao, Q., and B. Geerts, 2007: Fine-scale vertical structure and dynamics of some dryline boundaries observed in IHOP. *Mon. Wea. Rev.*, **135**, 4161-4184.
- Michimoto, K., 1991: A study of radar echoes and their relation to lightning discharge of thunderclouds in the Hokuriku district. Part I: Observation and analysis of thunderclouds in summer and winter. *J. Meteor. Soc. Japan*, **69**, 327-335.
- Michimoto, K., 1993: A study of radar echoes and their relation to lightning discharges of thunderclouds in the Hokuriku District. Part II: Observation and analysis of "Single-Flash" thunderclouds in midwinter. *J. Meteor. Soc. Japan*, **71**, 195-204.
- Moisseev, D., L. Bliven, P. Saavedra, S. Lautaportti, A. Battaglia, V. Chandrasekar, 2012: Inference of dominating snow growth processes from radar observations. ERAD conference, Toulouse, France, 25-29 June.
- Moore, P. K., and R. E. Orville, 1990: Lightning characteristics in lake-effect thunderstorms. *Mon. Wea. Rev.*, **118**, 1767-1782.
- Moreau, E., E. Le Bouar, J. Testud, P. Tabary, S. Westrelin, P. Bernard, L. Merindol 2012: Snow algorithm for dual polarized X-band radar. ERAD conference, Toulouse, France, 25-29 June.
- Mourad, P.D., and R.A. Brown, 1990: Multiscale large eddy states in weakly stratified planetary boundary layers, *J. Atmos. Sci.* **47**, 414-438.
- National Weather Service Forecast Office, Buffalo, NY, cited 2009a: Lake effect storm Iron. [Available online at <http://www.erh.noaa.gov/buf/lakeeffect/lake0304/i/stormi.html>.]

- National Weather Service Forecast Office, Buffalo, NY, cited 2009b: Summary of lake effect snow event over the Tug Hill February 3-12, 2007. [Available online at [http://www.erh.noaa.gov/buf/locust/.](http://www.erh.noaa.gov/buf/locust/)]
- Newman, A. J., P. A. Kucera, and L. F. Bliven, 2009: Presenting the Snowflake Video Imager (SVI). *J. Atmos. Oceanic Technol.*, **26**, 167-179.
- Niziol, T.A., W.R. Snyder, and J.S. Waldstreicher, 1995: Winter weather forecasting throughout the Eastern United States. Part IV: Lake-effect snow. *Wea. Forecasting*, **10**, 61-77.
- Nesbitt, S. and co-authors, 2012: Multiple wavelength perspective of precipitation and drop size distribution characteristics in MC3E. ERAD conference, Toulouse, France, 25-29 June (oral presentation 5.5).
- Park, H., A.V. Ryzhkov, D.S. Zrnić, and K.E. Kim, 2009: The hydrometeor classification algorithm for the polarimetric WSR-88D: description and application to an MCS. *Wea. Forecasting*, **24**, 730-748.
- Parish, T.R., M.D. Burkhart, and A.R. Rodi, 2007: Determination of the horizontal pressure gradient force using global positioning system on board an instrumented aircraft. *J. Atmos. Oceanic Technol.*, **24**, 521-528.
- Perovich, D.K., W. Meier, J. Maslanik, and J. Richter-Menge, 2012: Trend in Arctic sea ice cover. Section 5.i in State of the Climate 2011, Special Supplement, *Bull. Amer. Meteor. Soc.*, **93**, S140-142.
- Peace, R. L., R. B. Sykes, 1966: Mesoscale study of a lake effect snow storm. *Mon. Wea. Rev.*, **94**, 495-507.
- Potvin, C., A. Shapiro, M. Biggerstaff, J. Wurman, 2011: The VDAC technique: a variational method for detecting and characterizing convective vortices in multiple-Doppler radar data, *Mon. Wea. Rev.*, **139**, 2593-2613.
- Rasmussen, R.M., J. Hallett, R. Purcell, and S. Landolt, and J. Cole, 2011: The hotplate precipitation gauge. *J. Atmos. Oceanic Technol.*, **28**, 148-164.
- Rasmussen, R., and co-authors, 2012: How well are we measuring snow: the NOAA/FAA/NCAR Winter Precipitation test bed. *Bull. Amer. Meteor. Soc.*, **93**, 811-829.
- Rauber, R.M., and Co-authors, 2007: In the driver's seat: RICO and education. *Bull. Amer. Meteor. Soc.*, **88**, 1929-1937.
- Rauber, R.M., G.M. McFarquhar, B.F. Jewett, K.R. Knupp, D. Leon, P.S. Market, D.M. Plummer, J.M. Keeler, A. Rosenow, J. Wegman, M. Peterson, R. Wade, and K. Crandall, 2012: Rediscovering instability in winter storms. *Bull. Amer. Meteor. Soc.*, in revision.
- Reinking, R. F., R. Caiazza, R. Kropfli, B. Orr, B. Martner, T. Niziol, G. Byrd, R. Penc, R. Zamora, J. Snider, R. Ballentine, A. Stamm, C. Bedford, P. Joe and A. Koscielny, 1993: The Lake Ontario Winter Storms (LOWS) project. *Bull. Amer. Meteor. Soc.*, **74**, 1828-1849.
- Reynolds, S. E., M. Brook, and M. F. Gourley, 1957: Thunderstorm charge separation. *J. Atmos. Sci.*, **14**, 426-436.
- Rodriguez, Y., D.A.R. Kristovich, and M.R. Hjelmfelt, 2007: Lake-to-lake cloud bands: frequencies and locations. *Mon. Wea. Rev.*, **135**, 4202-4213.
- Rotunno, R., J. B. Klemp, and M. L. Weisman, 1988: A theory for strong, long-lived squall lines. *J. Atmos. Sci.*, **45**, 463-485.
- Ryzhkov, A. and D. S. Zrnic, 1998: Discrimination between rain and snow with a polarimetric radar. *J. Appl. Meteor.*, **37**, 1228-1240.
- Ryzhkov, A., D. S. Zrnic, and B. A. Gordon, 1998: Polarimetric method for ice water content determination. *J. Appl. Meteor.*, **37**, 125-134.

- Ryzhkov, A.V., S.E. Giangrande, and T.J. Schuur, 2005: Rainfall estimation with a polarimetric prototype of the WSR-88D radar. *J. Appl. Meteor.*, **44**, 502 - 515.
- Sang, J.G., 1993: On the dynamics of convection waves. *Q. J. R. Meteorol. Soc.*, **119**, 715-732.
- Schneebeil, M., 2012: Observation of high resolution vertical profiles of X-band weather radar observables during snowfall in the Swiss Alps. ERAD conference, Toulouse, France, 25-29 June.
- Schroeder, J.J., D.A.R. Kristovich, and M.R. Hjelmfelt, 2006: Boundary layer and microphysical influences of natural cloud seeding on a lake-effect snow storm. *Mon. Wea. Rev.*, **134**, 1842-1858.
- Schultz, D. M., 1999: Lake-effect snowstorms in northern Utah and western New York with and without lightning. *Wea. Forecasting*, **14**, 1023-1031.
- Shi, J. J., and Co-authors, 2010: WRF Simulations of the 20-22 January 2007 snow events over Eastern Canada: comparison with in situ and satellite observations. *J. Appl. Meteor. Climatol.*, **49**, 2246-2266.
- Skamarock, W. C., and Coauthors, 2008: A description of the advanced research WRF version 3. NCAR Tech. Note NCAR/ TN-4751STR, 88 pp.
- Snyder, Jeffrey C., Howard B. Bluestein, Guifu Zhang, Stephen J. Frasier, 2010: Attenuation correction and hydrometeor classification of high-resolution, x-band, dual-polarized mobile radar measurements in severe convective storms. *J. Atmos. Oceanic Technol.*, **27**, 1979-2001.
- Spinar, M.L., and D. A. R. Kristovich 2007: Multiscale interactions in a lake-effect snowstorm. AMS 12th conference on Mesoscale Processes, Waterville NH, 6-9 Aug 2007 [available at <https://ams.confex.com/ams/12meso/webprogram/Paper126160.html>].
- Steiger, S. M., R. Hamilton, J. Keeler, and R. E. Orville, 2009: Lake-effect thunderstorms in the lower Great Lakes. *J. Appl. Meteor. Clim.*, **48**, 889-902.
- Steiger et al. 2012: Circulations, bounded weak echo regions, and horizontal vortices observed by the Doppler on Wheels during long lake-axis-parallel lake-effect storms over Lake Ontario during the winter of 2010-11. In preparation for *Mon. Wea. Rev.*
- Stroeve, J.C., and co-authors, 2012: The Arctic's rapidly shrinking sea ice cover: a research synthesis. *Climatic Change*, **110**, 1005-1027, DOI: 10.1007/s10584-011-0101-1.
- Takahashi, T., 1978: Riming electrification as a charge generation mechanism in thunderstorms. *J. Atmos. Sci.*, **35**, 1536-1548.
- Toth, M., R. J. Trapp, J. Wurman, K. A. Kosiba, 2012: Improving tornado intensity estimates with Doppler radar. Submitted to *Wea. Forecasting*.
- Tripoli, G.J., 2005: Numerical study of the 10 January 1998 lake-effect bands observed during Lake-ICE. *J. Atmos. Sci.*, **62**, 3232-3249.
- Vali, G., and A. Rodi, 2005: Co-location of aircraft and radar data. Unpublished work available [here](#).
- Vivekanandan, J., V. N. Bringi, M. Hagen, and P. Meischner, 1994: Polarimetric radar studies of atmospheric ice particles. *IEEE Trans. Geosci. Remote Sens.*, **32**, 1-10.
- Vivekanandan, J., S.M. Ellis, R. Oye, D.S. Zrnić, A.V. Ryzhkov, and J. Straka, 1999: Cloud microphysics retrieval using S-band dual-polarization radar measurements. *Bull. Amer. Meteor. Soc.*, **80**, 381-388.
- Wade, R. and K. Knupp, 2012: A kinematic and microphysical analysis of a thundersnow event during PLOWS. *Mon. Wea. Rev.* (in preparation, submission expected August 2012)
- Wakimoto, R. M. and J. W. Wilson, 1998: Non-supercell tornadoes. *Mon. Wea. Rev.*, **117**, 1113-1140.

- Wakimoto, R. M., Atkins N. T., and J. Wurman, 2011: The LaGrange tornado during VORTEX2. Part I: Photogrammetric Analysis of the Tornado Combined with Single-Doppler Radar Data. *Mon. Wea. Rev.*, **139**, 2233-2258.
- Wakimoto, R.M., P. Stauffer, W.-C. Lee, N. Atkins, J. Wurman, 2012: Finescale structure of the LaGrange, Wyoming tornado during VORTEX2: GBVTD and photogrammetric analyses. *Mon. Wea. Rev.*, In Press, <http://dx.doi.org/10.1175/MWR-D-12-00036.1>.
- Walter, B.A., and J.E. Overland, 1984: Observations of longitudinal rolls in a near neutral atmosphere. *Mon. Wea. Rev.* **112**, 200-208.
- Wang, T.A., and Y.L. Lin, 1999: Wave ducting in a stratified shear flow over a two-dimensional mountain. Part I: General linear criteria. *J. Atmos. Sci.*, **56**, 412-436.
- Wang, Y., and B. Geerts, 2009: Estimating the evaporative cooling bias of an airborne reverse flow thermometer. *J. Atmos. Ocean. Tech.*, **26**, 3-21.
- Wang, Y., B. Geerts, and J. French, 2009: Dynamics of the cumulus cloud margin: an observational study. *J. Atmos. Sci.*, **66**, 3660-3677.
- Wang, Y., and B. Geerts, 2010: Humidity variations across the edge of trade wind cumuli: observations and dynamical implications. *Atmos. Res.*, **97**, 144-156. doi:10.1016/j.atmosres.2010.03.017.
- Wang, Y., and B. Geerts, 2011: Observations of detrainment patterns from non-precipitating orographic cumulus clouds. *Atmos. Res.*, **99**, 302-324.
- Wang, Y. and B. Geerts, 2012: Composite vertical structure of vertical velocity in shallow cumulus clouds. *Mon. Wea. Rev.*, in print.
- Wang, Z., and Co-authors, 2012: Single aircraft integration of remote sensing and in situ sampling for the study of cloud microphysics and dynamics. *Bull. Amer. Meteor. Soc.*, **93**, 653-668.
- Wang, Y., and V. Chandrasekar, 2010: Quantitative precipitation estimation in the CASA X-band Dual-Polarization Radar network. *J. Atmos. Oceanic Technol.*, **27**, 1665-1676.
- Weckwerth, T.M., D.B. Parsons, S.E. Koch, J.A. Moore, M.A. LeMone, B.B. Demoz, C. Flamant, B. Geerts, J. Wang, and W.F. Feltz, 2004: An overview of the International H₂O Project (IHOP_2002) and some preliminary highlights. *Bull. Amer. Meteor. Soc.*, **85**, 253-277.
- Weisman, M. L., J. B. Klemp, 1982: The dependence of numerically simulated convective storms on vertical wind shear and buoyancy. *Mon. Wea. Rev.*, **110**, 504-520.
- Weisman, M. L., J. B. Klemp, 1984: The structure and classification of numerically simulated convective storms in directionally varying wind shears. *Mon. Wea. Rev.*, **112**, 2479-2498
- Winstead, N. S., R. M. Schaaf, and P. D. Mourad, 2001: Synthetic Aperture Radar observations of the surface signatures of cold-season bands over the Great Lakes. *Wea. Forecasting*, **16**, 315-328.
- Wolfe, J.P., J.R. Snider and B. Geerts, 2008: Development of a temperature-dependent radar reflectivity to snowrate relationship for the S-band. Presented at the 15th International Conference on Clouds and Precipitation, Cancun, Mexico, July 2008.
- Wurman, J. M., 2001: The DOW Multiple-Doppler Network. Preprints, 30th Int. Conf. On Radar Meteorology, Munich, Germany, Amer. Meteor. Soc., 95-97.
- Wurman, J., 2010a: The challenge of observing small-scale phenomena. *Meteor. Tech. Inter.*, **1**, 66-71.
- Wurman, J., 2010b: Integration of technologies to collect tornado data. *Meteor. Tech. Inter.*, **2**, 22-25.

- Wurman., J., K. Kosiba, P. Markowski, Y. Richardson, D. Dowell, P. Robinson, 2010: Fine-scale single- and dual-Doppler analysis of tornado intensification, maintenance, and dissipation in the Orleans, Nebraska, tornadic supercell., *Mon. Wea. Rev.*, **138**, 4439-4455.
- Wurman, J., D. Dowell, Y. Richardson, P. Markowski, E. Rasmussen, D. Burgess, L. Wicker, and H. Bluestein, 2012: Verification of the Origins of Rotation in Tornadoes Experiment 2: VORTEX. *Bull. Amer. Meteor. Soc.*, in press, <http://dx.doi.org/10.1175/BAMS-D-11-00010.1>.
- Wurman, J., K. A. Kosiba, P. Robinson, 2013: In-Situ, Doppler Radar and Video Observations of the Interior Structure of a Tornado and Wind-Damage Relationship. Submitted to *Bull. Amer. Meteor. Soc.*
- Yang, Q., and B. Geerts, 2006: Horizontal convective rolls in cold air over water: buoyancy characteristics of coherent plumes detected by an airborne radar. *Mon. Wea. Rev.*, **134**, 2373-2396.
- Young, G.S., D.A.R. Kristovich, M.R. Hjelmfelt, and R.C. Foster, 2002: Rolls, streets, waves, and more: a review of quasi-two-dimensional structures in the atmospheric boundary layer. *Bull. Amer. Meteor. Soc.*, **83**, 997-1001.
- Zajac, B. A. and J. F. Weaver, 2002: Lightning Meteorology I: An Introductory Course on Forecasting with Lightning Data. Preprints, *Symposium on the Advanced Weather Interactive Processing System (AWIPS)*, Orlando, FL, Amer. Meteor.Soc., J8.6.
- Zrnić, D. S., and A. Ryzhkov, 1996: Advantages of rain measurements using specific differential phase. *J. Atmos. Oceanic Technol.*, **13**, 454-464.
- Zrnić, D.S., and A.V. Ryzhkov, 1999: Polarimetry for Weather Surveillance Radars. *Bull. Amer. Meteor. Soc.*, **80**, 389-406.